

CONFIDENTIAL

Copy
RM L52G18a

NACA RM L52G18a



RESEARCH MEMORANDUM

AERODYNAMIC LOAD MEASUREMENTS OVER A LEADING-EDGE SLAT ON
40° SWEEPBACK WING AT MACH NUMBERS FROM 0.10 TO 0.91

By Jones F. Cahill and Robert J. Nuber

Langley Aeronautical Laboratory
Langley Field, Va.

FOR REFERENCE

NOT TO BE TAKEN FROM THIS ROOM

CLASSIFIED DOCUMENT

This material contains information affecting the National Defense of the United States within the meaning of the espionage laws, Title 18, U.S.C., Secs. 793 and 794, the transmission or revelation of which in any manner to unauthorized person is prohibited by law.

NATIONAL ADVISORY COMMITTEE
FOR AERONAUTICS

WASHINGTON
September 23, 1952

CONFIDENTIAL

LIBRARY

THE NATIONAL ADVISORY COMMITTEE FOR AERONAUTICS
Langley Field, Va.

CLASSIFICATION CANCELLED

Authority: NACA L52G18a, 1-10-52

RM-104

By: J. F. Cahill, R. J. Nuber

See



NATIONAL ADVISORY COMMITTEE FOR AERONAUTICS

RESEARCH MEMORANDUM

AERODYNAMIC LOAD MEASUREMENTS OVER A LEADING-EDGE SLAT ON

A 40° SWEEPBACK WING AT MACH NUMBERS FROM 0.10 TO 0.91

By Jones F. Cahill and Robert J. Nuber

SUMMARY

An investigation of the aerodynamic loads on a leading-edge slat on a 40° sweptback wing having NACA 64₁-112 airfoil sections normal to the 0.273-chord line has been made in the Langley low-turbulence pressure tunnel. Load data for the slat in the retracted configuration were obtained from pressure-distribution measurements, whereas those for the slat in the extended configuration were obtained from a strain-gage balance on which the slat was mounted. Data were obtained for angles of attack from zero lift to nearly maximum lift for several Mach numbers from 0.10 to 0.91. Some lift and drag measurements for the complete wing were also made.

Increasing the Mach number from 0.10 to 0.84 had little effect on slat normal-force coefficients at any given wing lift coefficient and had little effect on slat chord-force coefficients at low wing lift coefficients. At higher wing lift coefficients (above about 0.5), increasing the Mach number caused a decrease in the magnitude of the negative chord-force coefficient as a result of a loss in the leading-edge suction force. Between Mach numbers of 0.84 and 0.91, both slat normal-force and slat chord-force coefficients decreased abruptly.

INTRODUCTION

In order to increase the naturally low maximum lift coefficients and improve the stability characteristics of the thin swept wings used on high-speed aircraft, leading-edge slats are being used for some high-speed flight conditions as well as for the landing condition. Automatically operating slats have been incorporated in a number of airplane designs since they relieve the pilot of the necessity for manual operation. The available information on the loads to be expected on leading-edge slats, however, is limited primarily to low-speed two-dimensional data. Since the available wing theory is not sufficiently

developed to take into account quantitatively the large flow changes caused by compressibility effects and wing sweep for a configuration as complex as a wing with a leading-edge slat, very little is known about the loads on leading-edge slats or about the force available to provide automatic operation of the slats on swept wings at high speeds.

An investigation has been made, accordingly, in the Langley low-turbulence pressure tunnel to determine the air loads over a retracted and extended leading-edge slat at Mach numbers up to 0.91. A 40° swept-back wing having NACA 64₁-112 airfoil sections perpendicular to the 0.273-chord line was employed in the investigation. The tests included lift and pressure-distribution measurements at five spanwise stations for the wing alone (to simulate the wing with a retracted slat) and wing lift and drag and slat normal and chord forces with the slat extended. The Reynolds number was held constant at a value of approximately 3×10^6 for all tests.

SYMBOLS

α	angle of attack
C_L	wing lift coefficient, $\frac{L}{qS_w}$
C_D	wing drag coefficient, $\frac{D}{qS_w}$
C_C	slat chord-force coefficient, $\frac{C}{qS_s}$
C_N	slat normal-force coefficient, $\frac{N}{qS_s}$
C_{m_s}	slat-pitching-moment coefficient, $\frac{M'}{qS_s c_s}$
C_R	slat resultant-force coefficient, $(C_C^2 + C_N^2)^{1/2}$
θ	inclination of slat resultant-force vector, $\tan^{-1}\left(\frac{-C_C}{C_N}\right)$
S	pressure coefficient, $\frac{H_o - p}{q}$
S_{cr}	critical pressure coefficient

L	lift on semispan wing
D	drag on semispan wing
C	slat chord force in the wing chord plane, perpendicular to wing leading edge, positive to rear
N	slat normal force perpendicular to wing chord plane, positive upward
M'	slat pitching moment about slat quarter-chord axis
c	chord parallel to plane of symmetry
c'	chord perpendicular to wing leading edge
$c^*/4$	quarter chord of unswept wing
c_s	slat chord perpendicular to wing leading edge
$b/2$	wing semispan
h	chordwise distance from slat leading edge to slat center of pressure, perpendicular to wing leading edge
x	perpendicular distance from wing leading edge, positive to rear
y	perpendicular distance outboard from plane of symmetry
z	perpendicular distance from chord plane, positive upward
S_w	wing semispan area
S_s	slat area
H_o	stream total pressure
q	stream dynamic pressure
p	local static pressure
M	stream Mach number

DESCRIPTION OF MODEL AND TESTS

The plan and profile views of the semispan wing are shown in figure 1. The wing sweep, defined as the sweep angle of the quarter-chord line of an equivalent unswept wing, was 40° . This quarter-chord line becomes the 0.273-chord line of the swept wing measured parallel to the plane of symmetry. The wing, composed of NACA 64₁-112 airfoil sections perpendicular to the 0.273-chord line, had no geometrical twist, an aspect ratio of 4, and a taper ratio of 0.625. The airfoil sections were approximately 9 percent thick in the stream direction. This is the same model as described in reference 1, with the exception of the pressure orifices that were installed in the wing at five spanwise stations in lines perpendicular to the leading edge. At each spanwise station, the orifices extended from 0.050c' on the lower surface around the leading edge to 0.250c' on the upper surface. The location of these orifices is shown in figure 1(b). The orifices were connected to a multiple-tube manometer and the pressures were recorded photographically.

Photographs of the model with the slat extended are shown in figure 2. The slat had a constant chord of 2.01 inches (0.22 wing chord parallel to the plane of symmetry at the midspan of the slat) and a span of 0.575 wing semispan beginning at 0.40 wing semispan. The slat was attached to the wing by means of three strain-gage beams which were used to measure the slat forces. This slat configuration is somewhat similar to the configuration for which data are presented in reference 2. The slat used for the investigation reported in reference 2 was tapered in plan form, having a chord of 22 percent of the local wing chord at all spanwise stations. In order to simplify the construction of the slat for the present investigation, the slat was made with a constant chord. To maintain some similarity with the slat of reference 2, the gap between the airfoil upper surface and the slat trailing edge (0.04c) and the chordwise distance between the airfoil leading edge and the slat trailing edge (0.013c) were fixed at the values used on the model of reference 2 (see fig. 1). The half-span split flap had a chord equal to 18.4 percent of the local wing chord and was deflected 60° about its hinge line.

The model was mounted on an electric resistance-type strain-gage semispan balance. For the wing alone (retracted slat), lift and pressure-distribution data were recorded for a range of angle of attack from zero lift to about maximum lift for Mach numbers of 0.10, 0.40, 0.60, 0.70, 0.80, 0.84, and 0.91. For the wing with the slat extended, lift and drag on the wing and slat normal and chord forces were measured for a range of angle of attack from zero lift to about maximum lift for Mach numbers of 0.20, 0.39, 0.59, 0.69, 0.80, and 0.91. Similar data were obtained for the wing with the half-span trailing-edge flap

deflected individually at a Mach number of 0.10 and in combination with the leading-edge slat at a Mach number of 0.20.

All tests were made at a Reynolds number of approximately 3×10^6 . Jet boundary corrections to the angle of attack were applied by using the method described in reference 3. The coefficients and Mach numbers were corrected for tunnel-blocking effects by a method based on information presented in references 4 and 5.

The tests at Mach numbers of 0.10 and 0.20 were made in air whereas all those at higher Mach numbers were made using Freon-12 as a testing medium. The values of the coefficients and Mach numbers as obtained in Freon-12 were converted to corresponding values in air by the methods presented in reference 6.

RESULTS AND DISCUSSION

Wing Force Data

Force data for the wing alone and with the slat extended are presented in figures 3 to 5. Extension of the slat is shown to cause relatively small increases in maximum lift (approximately 0.1). The lift data shown in figures 3 and 4 are in very good agreement with the data of reference 2 in the linear lift range but the maximum lift coefficients are lower than those of reference 2 by about 0.05 for the plain wing and for the wing with both the flap and slat extended, and by about 0.1 for the wing with the flap deflected alone. Increasing the Mach number up to 0.70 caused a slight decrease in maximum lift, both for the wing alone and with the slat extended. The drag coefficients shown in figure 5 are about 0.01 higher than those of reference 2 at low lift coefficients. This difference decreases gradually as the lift coefficient is increased and the agreement is very good for lift coefficients just below the stall. Data presented in reference 2 show that this slat is effective in improving the longitudinal stability of this wing at maximum lift at low speeds. No pitching-moment data were obtained in the present investigation.

Slat Force Data

Force data for the retracted slat are presented in figure 6 and for the extended slat in figure 7. The forces for the slat-retracted configuration were obtained from integration of the pressure-distribution results of table I using the assumption that the pressure on the enclosed lower surface of the slat is equal to the pressure at the lower-surface juncture of the slat and wing. Data presented in

reference 7 show that this assumption is justified. It is possible that, for some other configuration, the pressure on this enclosed surface could attain some other value, depending on the location and effectiveness of seals between the wing and slat. These pressure distributions were integrated over an area equal to the area covered by the extended slat (constant chord of 2.01 inches from $0.40b/2$ to $0.975b/2$). Loads over a slat of any other size within the area covered by the pressure orifices can be obtained by using the proper limits for the integration. Forces for the slat-extended conditions were obtained from strain-gage balance readings. An examination of figures 6 and 7 shows that the variations with lift coefficient and with Mach number of both the normal-force and chord-force coefficients for the slat in the open condition are, in general, similar to those for the closed condition.

Slat normal-force coefficients increase almost linearly as the wing lift coefficient is increased, reaching a maximum value at 75 to 80 percent of maximum lift. Further increases in wing lift coefficient cause the slat normal-force coefficients to decrease. At negative normal-force coefficients there is a decided change in the slope of the slat-extended normal-force curve caused by separation of the flow from the lower surface of the slat. It should be noted that extension of the slat results in a decrease of about 0.7 in slat normal-force coefficient. Deflection of the trailing-edge flap causes a reduction in slat normal-force coefficient at low values of wing lift coefficient, but the increase of slat normal force with increasing wing lift continues to higher wing lift coefficients. The maximum values of normal-force coefficient of the retracted slat were 2.0 with the flap retracted and 2.1 with the flap deflected. The maximum normal-force coefficient on the extended slat was 1.8 for the flap both retracted and deflected.

Increases in Mach number from 0.10 to 0.84 appear to have little effect on slat normal-force coefficient, either extended or retracted, except at the highest lift coefficients. At lift coefficients higher than 0.75 the slat normal-force coefficient is somewhat higher at a Mach number of 0.10 than at other speeds. At a Mach number of 0.91, however, the slat normal-force coefficient is reduced from the lower Mach number values at all lift coefficients.

All the retracted-slat force and moment values depend on the assumption made concerning the pressure on the enclosed slat lower surface. The greatest change in slat loads from those for the assumed conditions would be for a case where the pressure on the enclosed surface is equal to the pressure at the upper-surface juncture of the slat and wing. If that condition were realized, the maximum values of slat normal-force coefficient for the retracted slat would be 0.84 and 0.96 for the trailing-edge flap retracted and extended, respectively. It is of interest to note in this connection that, for small openings of the slat, when the seal just opens, the load distribution over the slat

should be similar to those used to obtain the data of figure 6 with the exception that the pressures on the enclosed lower surface of the slat would vary along the surface from the value at the lower-surface juncture to the value at the upper-surface juncture. Both the normal-force and the chord-force coefficients would therefore be lower than shown in figure 6.

The chord forces are in the forward direction for wing lift coefficients above about 0.2 for the slat-retracted condition and above about 0.3 for the slat-extended condition. Increases in wing lift coefficient cause the slat chord-force coefficient to increase in the forward direction for wing lift coefficients up to about 0.7 or 0.8 and, in general, to decrease for lift coefficients above this value. At a given wing lift coefficient below the value at which the reversal in slat chord-force variation occurs, deflection of the trailing-edge flap causes a decrease in the magnitude of the negative chord-force coefficient. The chord force continues to increase up to a higher lift coefficient, however, and the maximum chord-force coefficient is higher with the flap deflected than with the flap retracted. Maximum values of chord force for the trailing-edge flap-retracted and flap-deflected conditions, respectively, were -0.96 and -1.17 with the slat retracted and -0.60 and -0.65 with the slat extended. The maximum values of the chord-force coefficient for the slat retracted would be reduced to -0.474 and -0.692 for the flap retracted and extended, respectively, if the pressure on the enclosed surface were decreased to the value existing at the upper-surface juncture of the wing and slat.

The chord-force coefficients are little affected by changes in Mach number at low lift coefficients. At lift coefficients above about 0.5, however, increases in Mach number up to 0.60 cause a decrease in the negative chord-force coefficient. Between Mach numbers of 0.60 and 0.84 very little change is encountered, but a large decrease in the negative value of the chord-force coefficient is caused by an increase in Mach number from 0.84 to 0.91. The variations in chord-force coefficient caused by changes in Mach number and angle of attack are less pronounced for the slat-extended condition than for the slat-retracted condition.

Resultant-force coefficients and the inclination of the resultant-force vector for the slat in the retracted condition are shown in figure 8. For lift coefficients below about 0.65, the magnitude of the resultant-force coefficient is little affected by changes in Mach number up to 0.84. Increasing the Mach number from 0.84 to 0.91 causes a sharp decrease in the resultant-force coefficient. At lift coefficients above 0.65 an increase in Mach number causes the resultant-force coefficient to decrease even for low values of Mach number as a result of the previously shown changes in chord-force coefficient. The inclination of the resultant-force vector decreases as the Mach number is increased from 0.10 to about 0.70, remains constant for Mach numbers from 0.70 to 0.84, and then decreases further as the Mach number is increased to 0.91. As

a result of these variations in the resultant-force vectors, the operation of leading-edge slats can be affected by changes in Mach number whether the slats are designed to extend when the magnitude of the slat load exceeds a specified value or when the slat-load vector is inclined forward of a specified angle. The manner in which the slats operate and the specific values of slat load or slat-load inclination which cause the slat to open depend, of course, on the detail design of the slat.

Data for the slat pitching moments are available from the pressure distributions measured for the slat-retracted condition. These pitching moments are shown in figure 6 and the chordwise positions of the slat center of pressure are shown in figure 9. At low lift coefficients, the center of pressure is at approximately 47 percent of the slat chord for low Mach numbers and moves to the rear as the Mach number is increased, reaching 51 percent of the chord at a Mach number of 0.91. For low Mach numbers, increasing the lift-coefficient first causes the center of pressure to move forward at lift-coefficients up to that at which the chord force reaches its peak. At higher lift coefficients, the center of pressure moves rearward. For Mach numbers between about 0.70 and 0.84, the center of pressure moves continuously to the rear as the lift coefficient is increased.

Slat-Pressure Distributions

In view of the similarities which have been shown to exist in the variations of the slat forces with Mach number and angle of attack for the slat in the retracted and extended conditions, it seems likely that the changes in flow phenomena about the slat in these two conditions would also be similar. The following discussion of the pressure-distribution data obtained for the slat-retracted condition can probably be considered to apply at least qualitatively also to pressure distributions for the slat-extended condition. The pressure-distribution data are presented in table I. Some of these pressure-distribution data have previously been presented in reference 8.

Typical pressure-distribution plots are shown in figure 10 for several angles of attack. These data are of assistance in gaining an understanding of the variations of the normal-force and chord-force coefficients shown previously. At a low angle of attack (approximately 4°), only very small changes in the pressure distribution are caused by changes in Mach number. As a result, of course, the normal-force and chord-force coefficients are also unaffected by changes in Mach number. At the higher angles of attack, however, an increase in Mach number from 0.10 to 0.60 causes the peak pressure coefficient on the leading edge to be greatly reduced and the pressure coefficient on the rear portion of the slat to increase. The net result of these

changes is to cause the normal force to remain approximately constant. The chord force, on the other hand, becomes less negative as a result of the decrease in suction force at the leading edge. The rearward movement in the center-of-pressure position with increases in Mach number is also apparent from this change in pressure distribution.

An examination of the data in figure 10 shows that the large decrease in peak pressure coefficient at angles of attack above 4° occurs as the flow over the slat becomes supersonic. Data showing similar effects of increasing Mach number on peak pressure coefficients at high lift coefficients are shown in references 9 and 10 where the variation of maximum lift coefficient with Mach number is shown to be strongly affected by the existence of supersonic flows. No conclusive explanation can be offered for the change in slat loads between Mach numbers of 0.84 and 0.91, although this phenomenon seems to be associated with the fact that the pressures on the upper surface of the slat approach a complete vacuum at the higher Mach numbers. The normal-force coefficients shown in reference 7 show a similar but somewhat more gradual decrease between Mach numbers of approximately 0.8 and 0.88. It is also possible that proximity to tunnel choking conditions at a Mach number of 0.91 may have had an influence on the data obtained. The computed choking Mach number based on one-dimensional area-ratio considerations is approximately 0.95.

CONCLUSIONS

An investigation in the Langley low-turbulence pressure tunnel of the aerodynamic loads on a partial-span leading-edge slat on a 40° swept-back wing having NACA 64₁-112 airfoil sections perpendicular to the 0.273-chord line at Mach numbers up to 0.91 has indicated the following conclusions:

1. Increasing the Mach number from 0.10 to 0.84 had very little effect on slat normal-force coefficients at any given wing lift coefficient and had little effect on slat chord-force coefficients at low wing lift coefficients. At higher lift coefficients (above about 0.5), increasing the Mach number caused a decrease in the magnitude of the slat negative chord-force coefficient as a result of a loss in the leading-edge suction force.

2. Between Mach numbers of 0.84 and 0.91, both slat normal-force and slat chord-force coefficients decrease abruptly.

Langley Aeronautical Laboratory,
National Advisory Committee for Aeronautics,
Langley Field, Va.

REFERENCES

1. Cahill, Jones F.: Comparison of Semispan Data Obtained in the Langley Two-Dimensional Low-Turbulence Pressure Tunnel and Full-Span Data Obtained in the Langley 19-Foot Pressure Tunnel for a Wing With 40° Sweepback of the 0.27-Chord Line. NACA RM L9B25a, 1949.
 2. Graham, Robert R., and Conner, D. William: Investigation of High-Lift and Stall-Control Devices on an NACA 64-Series 42° Sweptback Wing With and Without Fuselage. NACA RM L7G09, 1947.
 3. Katzoff, S., and Hannah, Margery E.: Calculation of Tunnel-Induced Upwash Velocities for Swept and Yawed Wings. NACA TN 1748, 1948.
 4. Glauert, H.: Wind Tunnel Interference on Wings, Bodies and Airscrews. R. & M. No. 1566, British A.R.C., 1933.
 5. Herriot, John G.: Blockage Corrections for Three-Dimensional-Flow Closed-Throat Wind Tunnels, With Consideration of the Effect of Compressibility. NACA Rep. 995, 1950. (Supersedes NACA RM A7B28.)
 6. Von Doenhoff, Albert E., and Braslow, Albert L.: Studies of the Use of Freon-12 As a Testing Medium in the Langley Low-Turbulence Pressure Tunnel. NACA RM L51111, 1951.
 7. Kelly, John A., and Hayter, Nora-Lee F.: Aerodynamic Characteristics of a Leading-Edge Slat on a 35° Swept-Back Wing for Mach Numbers From 0.30 to 0.88. NACA RM A51H23, 1951.
 8. Cahill, Jones F., and Oberndorfer, Gale C.: Pressure Distributions Over a Retracted Leading-Edge Slat on a 40° Sweptback Wing At Mach Numbers up to 0.9. NACA RM L50L04a, 1951.
 9. Furlong, G. Chester, and Fitzpatrick, James E.: Effects of Mach Number and Reynolds Number on the Maximum Lift Coefficient of a Wing of NACA 230-Series Airfoil Sections. NACA TN 1299, 1947.
 10. Furlong, G. Chester, and Fitzpatrick, James E.: Effects of Mach Number up to 0.34 and Reynolds Number up to 8×10^6 on the Maximum Lift Coefficient of a Wing of NACA 66-Series Airfoil Sections. NACA TN 2251, 1950.
- CONFIDENTIAL

TABLE I.- PRESSURE COEFFICIENTS FOR THE 40° SWEEPBACK WING
AT DIFFERENT SPANWISE STATIONS AND ANGLES OF ATTACK

(a) $M = 0.10$, split flap off

$\frac{y}{b/2}$	Orifice number	Angle of attack, α , deg														
		-0.02	2.1	4.1	8.3	10.4	12.5	14.6	16.6	17.6	18.7	19.7	20.7	22.7	24.7	26.7
0.429	1	1.151	0.974	0.824	0.590	0.505	0.455	0.448	0.498	0.498	0.327	0.370	0.377	0.355	0.355	0.348
	2	1.123	.888	.704	.476	.434	.448	.498	.597	.647	.419	.426	.426	.448	.448	.462
	3	1.052	.768	.569	.469	.533	.704	.896	1.144	1.294	.789	.689	.697	.739	.768	.782
	4	.498	.704	1.002	2.864	4.293	5.928	7.214	9.204	10.100	3.660	2.466	2.395	2.310	2.253	2.168
	5	.967	1.336	1.820	3.106	4.122	4.911	4.726	5.721	6.070	2.601	2.409	2.317	2.232		
	6	1.095	1.365	1.699	2.310	2.864	3.355	3.532	4.080	4.279	2.630	2.402	2.317	2.239	2.168	2.111
	7	1.130	1.336	1.564	2.075	2.381	2.665	2.736	3.035	3.134	2.687	2.402	2.310	2.232	2.146	2.068
	8	1.180	1.315	1.471	1.784	1.969	2.139	2.139	2.338	2.388	2.758	2.395	2.310	2.225	2.146	2.061
	9	1.194	1.308	1.400	1.670	1.798	1.919	1.891	2.090	2.139	2.736	2.417	2.310	2.225	2.154	2.011
	10	1.237	1.322	1.393	1.564	1.663	1.727	1.692	1.791	1.891	2.580	2.488	2.367	2.260	2.168	2.075
.558	11	1.144	.960	.803	.569	.490	.448	.448	.398	.391	.391	.391	.391	.391	.377	.377
	12	1.109	.874	.689	.490	.448	.476	.498	.498	.448	.434	.426	.426	.448	.448	.462
	13	1.031	.725	.547	.498	.633	.860	1.144	1.095	.945	.768	.695	.711	.746	.789	.817
	14	.483	.675	1.180	3.255	4.833	6.553	7.910	7.264	5.274	2.758	2.139	2.090	2.047	2.075	2.011
	15	.945	1.343	1.848	3.312	4.542	4.769	4.975	4.179	2.985	2.658	2.125	2.090	2.047		
	16	1.080	1.372	1.741	2.488	3.049	3.532	3.731	3.085	2.438	2.559	2.104	2.061	2.004	1.976	1.919
	17	1.137	1.350	1.599	2.111	2.452	2.743	2.836	2.836	2.388	2.438	2.075	2.026	1.962	1.919	1.869
	18	1.187	1.336	1.493	1.827	2.026	2.203	2.239	2.736	2.388	2.324	2.047	2.004	1.955	1.898	1.848
	19	1.194	1.315	1.422	1.699	1.848	1.969	1.940	2.587	2.388	2.317	2.047	2.004	1.955	1.898	1.848
	20	1.215	1.315	1.407	1.628	1.741	1.834	1.841	2.289	2.338	2.353	2.061	2.019	1.962	1.905	1.855
	21	1.237	1.322	1.400	1.578	1.670	1.741	1.692	2.139	2.289	2.402	2.082	2.033	1.969	1.919	1.862
.688	22	1.144	.960	.803	.569	.490	.448	.448	.498	.498	.419	.412	.419	.398	.384	.391
	23	.803	.647	.519	.498	.540	.597	.597	.597	.597	.483	.483	.448	.498	.498	.512
	24	1.009	.697	.519	.533	.711	1.009	1.343	.746	.796	.711	.668	.682	.718	.746	.782
	25	.483	.675	1.237	3.461	5.153	6.951	8.358	2.289	2.239	2.011	1.812	1.770	1.720	1.670	1.649
	26		1.372	1.883	3.447		4.598	5.075	2.239	2.090	1.969	1.791	1.748	1.706	1.656	1.635
	27	1.095	1.407	1.784	2.601	3.177	3.682	3.881	2.239	2.139	1.962	1.786	1.748	1.706	1.656	1.635
	28	1.137	1.358	1.613	2.154	2.488	2.786	2.886	2.239	2.139	1.955	1.777	1.741	1.706	1.656	1.635
	29	1.208	1.329	1.443	1.713	1.869	1.990	1.990	2.239	2.090	1.955	1.777	1.734	1.706	1.670	1.649
	30	1.230	1.329	1.407	1.635	1.756	1.848	1.841	2.289	2.139	1.962	1.791	1.748	1.720	1.684	1.656
	31	1.244	1.329	1.407	1.592	1.748	1.756	1.741	2.289	2.189	1.976	1.798	1.763	1.734	1.692	1.663
	.817	32	1.123	.945	.803	.590	.519	.483	.547	.547	.547	.483	.476	.483	.469	.455
33		1.130	.874	.682	.462	.462	.498	.597	.497	.547	.462	.448	.448	.462	.462	.469
34		1.038	.732	.547	.498	.625	.839	1.144	.647	.597	.532	.562	.569	.675	.640	.675
35		.505	.775	1.386	3.625	5.281	6.987	8.309	1.940	1.940	1.692	1.557	1.528	1.514	1.521	1.549
36		.952	1.343	1.869	3.461	4.556	4.954	5.174	1.841	1.791	1.684	1.549	1.521	1.507	1.514	1.543
37		1.087	1.393	1.748	2.559	3.184	3.582	3.781	1.841	1.791	1.677	1.543	1.521	1.493	1.514	1.535
38		1.144	1.365	1.613	2.154	2.466	2.751	2.836	1.841	1.791	1.670	1.535	1.521	1.493	1.514	1.528
39		1.187	1.336	1.500	1.848	2.040	2.210	2.239		1.841	1.670	1.535	1.528	1.514	1.521	1.535
40		1.223	1.322	1.414	1.635	1.741	1.827	1.841	1.841	1.841	1.677	1.549	1.535	1.528	1.528	1.549
41																
.946		42	1.166	1.002	.860	.654	.618	.547	.597	.647	.647	.590	.576	.569	.569	.547
	43	1.151	.924	.746	.547	.590	.533	.647	.647	.647	.554	.533	.540	.569	.554	.569
	44	1.045	.768	.604	.533	.640	.817	1.095	.746	.697	.633	.618	.640	.675	.711	.746
	45	.512	.597	.960	2.594	3.838	5.167	6.219	1.692	1.692	1.592	1.507	1.507	1.493	1.493	1.500
	46	.995	1.350	1.812	3.141	4.250	5.018	4.726	1.642	1.642	1.493	1.414	1.414	1.414	1.457	1.485
	47	1.137	1.379	1.684	2.345	2.772	3.220	3.433		1.642	1.478	1.414	1.414	1.414	1.457	1.485
	48	1.159	1.350	1.564	2.040	2.310	2.544	2.637	1.642	1.592	1.493	1.407	1.414	1.422	1.457	1.478
	49	1.187	1.315	1.457	1.741	1.905	2.040	2.040		1.592	1.493	1.414	1.422	1.429	1.457	1.478
	50	1.201	1.294	1.393	1.613	1.741	1.827	1.841	1.642	1.642	1.493	1.422	1.422	1.429	1.457	1.485
	51	1.215	1.294	1.379	1.557	1.649	1.706	1.692	1.642	1.642	1.507	1.422	1.422	1.436	1.464	1.493
	52	1.230	1.294	1.372	1.514	1.585	1.621	1.642	1.642	1.592	1.514	1.429	1.429	1.443	1.464	1.493

TABLE I.- PRESSURE COEFFICIENTS - Continued

(b) M = 0.10, split flap on

y b/2	Orifice number	Angle of attack, α, deg													
		-8.1	-6.0	-3.9	-1.9	4.4	8.6	10.6	12.7	13.7	14.8	15.8	16.8	18.8	20.8
0.429	1	1.521	1.336	1.151	0.974	0.604	0.469	0.427	0.448	0.398	0.498	0.320	0.370	0.370	0.363
	2	1.869	1.464	1.173	.931	.505	.448	.498	.597	.597	.647	.398	.419	.441	.448
	3	2.090	1.571	1.166	.824	.462	.647	.867	1.144	1.194	1.294	.746	.668	.697	.739
	4	1.393	.782	.505	.505	2.331	5.238	7.157	8.408	9.154	9.751	3.433	2.395	2.281	2.324
	5	.469	.583	.810	1.137	2.779	4.804	4.868	5.323	5.672	5.920	2.445	2.303	2.168	2.075
	6	.583	.739	.959	1.208	2.281	3.170	3.738	3.930	4.080	4.229	2.459	2.296	2.161	2.068
	7	.725	.867	1.038	1.230	1.976	2.594	2.928	2.985	3.035	3.184	2.473	2.296	2.168	2.075
	8	.867	.995	1.116	1.272	1.755	2.132	2.338	2.338	2.388	2.438	2.516	2.296	2.161	2.082
	9	.952	1.059	1.173	1.294	1.670	1.954	2.104	2.139	2.139	2.139	2.551	2.296	2.161	2.090
	10	1.073	1.166	1.244	1.343	1.628	1.827	1.912	1.841	1.891	1.940	2.509	2.324	2.182	2.097
.558	11	1.542	1.350	1.144	.960	.583	.469	.455	.498	.398	.299	.398	.405	.405	.405
	12	1.457	1.166	.917	.498	.476	.547	.547	.647	.448	.498	.455	.448	.462	.476
	13	2.139	1.578	1.137	.796	.490	.810	1.123	1.443	.945	.945	.803	.732	.768	.870
	14	1.215	.689	.483	.569	2.779	5.970	8.045	9.353	5.871	5.124	3.241	2.345	2.232	2.217
	15	.476	.590	.803	1.166	2.978	4.563	5.423	5.871	3.284	2.786	2.864	2.267	2.196	2.182
	16	.590	.746	.959	1.244	2.296	3.419	3.994	4.179	2.786	2.289	2.630	2.225	2.097	2.047
	17	.725	.874	1.052	1.258	2.040	2.694	3.049	3.134	2.637	2.239	2.409	2.146	2.011	1.969
	18	.874	1.002	1.137	1.294	1.812	2.217	2.438	2.438	2.687	2.239	2.288	2.047	1.976	1.940
	19	.945	1.059	1.173	1.301	1.704	2.018	2.182	2.189	2.587	2.239	2.260	2.026	1.969	1.933
	20	1.009	1.109	1.208	1.329	1.663	1.912	2.040	2.040	2.388	2.239	2.267	2.018	1.962	1.933
	21	1.073	1.158	1.251	1.350	1.649	1.848	1.947	1.891	2.289	2.239	2.274	2.018	1.969	1.940
.688	22	1.606	1.399	1.187	.995	.604	.483	.462	.547	.498	.498	.434	.441	.441	.441
	23	1.517	1.166	.917	.517	.517	.554	.604	.697	.647	.547	.519	.512	.533	.547
	24	2.260	1.656	1.173	.512	.512	.924	1.301	1.692	.846	.796	.732	.704	.746	.789
	25	1.343	.760	.498	.540	2.878	6.233	8.436	9.801	2.239	2.090	2.026	1.869	1.812	1.798
	26	.490	.604	.817	1.173	2.978	4.278	5.309	5.721	2.189	1.990	1.990	1.834	1.791	1.777
	27	.590	.739	.959	1.251	2.374	3.532	4.143	4.328	2.189	2.040	1.983	1.827	1.784	1.770
	28	.711	.867	1.045	1.258	2.054	2.822	3.106	3.184	2.189	2.040	1.983	1.819	1.777	1.770
	29	.945	1.059	1.173	1.301	1.712	2.026	2.196	2.189	2.239	2.040	1.962	1.805	1.777	1.770
	30	1.016	1.109	1.208	1.322	1.663	1.919	2.054	2.040	2.239	2.040	1.962	1.812	1.784	1.777
	31	1.066	1.151	1.244	1.336	1.635	1.848	1.954	1.891	2.239	2.040	1.962	1.812	1.784	1.777
	.817	32	1.642	1.443	1.237	1.045	.640	.525	.512	.597	.597	.547	.512	.519	.512
33		1.628	1.308	1.023	.540	.498	.498	.554	.647	.647	.547	.483	.483	.498	.505
34		2.345	1.755	1.294	.903	.498	.732	1.009	1.343	.697	.697	.604	.597	.640	.675
35		1.173	.697	.505	.569	2.807	5.991	8.081	9.353	1.990	1.841	1.755	1.663	1.677	1.670
36		.476	.561	.746	1.080	2.864	4.698	5.067	5.622	1.990	1.791	1.741	1.642	1.656	1.663
37		.569	.718	.924	1.201	2.324	3.376	3.973	4.129	1.990	1.791	1.741	1.635	1.656	1.656
38		.711	.853	1.023	1.230	2.004	2.658	2.999	3.085	1.990	1.791	1.720	1.628	1.649	1.649
39		.853	.981	1.109	1.258	1.777	2.189	2.409	2.488	1.990	1.791	1.713	1.620	1.642	1.649
40		.995	1.087	1.180	1.301	1.635	1.876	2.011	2.040	1.891	1.791	1.713	1.628	1.649	1.656
41		1.684	1.521	1.315	1.130	.746	.604	.569	.597	.647	.697	.625	.625	.611	.590
.946		42	1.118	1.684	1.379	1.109	.618	.540	.569	.647	.647	.697	.618	.590	.583
	43	2.367	1.812	1.372	.995	.519	.682	.896	1.194	.697	.746	.661	.668	.704	.411
	44	1.585	.959	.618	.498	1.791	4.087	5.643	6.716	1.841	1.741	1.741	1.699	1.692	1.635
	45	.519	.590	.746	1.038	2.509	4.421	5.164	4.876	1.741	1.642	1.599	1.564	1.571	1.556
	46	.597	.718	.924	1.123	2.999	2.885	3.461	3.632	1.692	1.592	1.556	1.564	1.564	1.549
	47	.753	.874	1.023	1.187	1.862	2.416	2.715	2.736	1.692	1.642	1.599	1.564	1.571	1.542
	48	.888	.995	1.102	1.230	1.649	1.990	2.168	2.189	1.692	1.642	1.599	1.556	1.564	1.542
	49	.967	1.052	1.137	1.237	1.564	1.819	1.947	1.990	1.741	1.692	1.599	1.556	1.571	1.542
	50	1.023	1.102	1.173	1.258	1.528	1.727	1.827	1.841	1.741	1.642	1.606	1.564	1.578	1.556
	51	1.066	1.130	1.194	1.272	1.514	1.663	1.748	1.741	1.741	1.692	1.606	1.564	1.585	1.564
	52	1.684	1.521	1.315	1.130	.746	.604	.569	.597	.647	.697	.625	.625	.611	.590

TABLE I.- PRESSURE COEFFICIENTS - Continued

(c) $M = 0.40$, split flap off

$\frac{y}{b/2}$	Orifice number	Angle of attack, α , deg							
		4.1	8.3	10.4	12.5	14.6	16.6	20.7	22.7
0.429	1	0.857	0.637	0.545	0.483	0.469	0.442	0.435	0.421
	2	.748	.542	.491	.465	.469	.442	.455	.473
	3	.616	.498	.546	.647	.650	.624	.636	.672
	4	.960	2.620	3.880	5.064	3.450	2.960	2.261	2.382
	5	1.837	3.130	4.085	4.872	2.915	2.506	2.143	2.062
	6	1.726	2.333	2.815	3.240	2.930	2.475	2.138	2.057
	7	1.587	2.105	2.345	2.646	2.950	2.475	2.138	2.069
	8	1.502	1.832	1.931	2.120	2.935	2.475	2.138	2.069
	9	1.473	1.710	1.741	1.919	2.590	2.506	2.143	2.074
	10	1.462	1.635	1.686	1.756	1.842	2.562	2.162	2.093
.558	11	.836	.618	.546	.471	.469	2.558	.429	.448
	12	.732	.530	.517	.471	.469	2.558	.473	.472
	13	.578	.524	.620	.722	.680	.652	.660	.697
	14	1.140	2.970	4.290	4.805	3.040	2.347	1.979	1.925
	15	1.867	3.360	4.525	-----	2.615	2.150	1.924	1.890
	16	1.767	2.520	3.010	3.880	2.615	2.124	1.919	1.884
	17	1.640	2.162	2.426	3.090	2.596	2.124	1.919	1.884
	18	1.520	1.878	2.040	2.205	2.640	2.708	1.919	1.877
	19	1.485	1.774	1.851	1.978	2.582	2.124	1.924	1.877
	20	1.468	1.675	1.797	1.902	2.323	2.124	1.930	1.890
	21	1.462	1.632	1.710	1.790	1.973	2.124	1.936	1.894
.688	22	.826	.604	.570	.517	.484	.511	.473	.463
	23	.640	.564	.570	.568	.567	.538	.546	.539
	24	.560	.550	.705	.730	.760	.670	.654	.693
	25	1.160	3.130	4.453	3.070	2.750	2.063	1.755	1.695
	26	1.908	3.535	4.016	2.700	2.395	1.868	1.696	1.652
	27	1.832	2.673	3.100	2.727	2.490	1.868	1.696	1.652
	28	1.657	2.205	2.494	2.748	2.490	1.837	1.696	1.696
	29	1.502	1.762	1.878	2.463	2.265	1.837	1.696	1.680
	30	1.479	1.690	1.798	2.032	2.164	1.837	1.708	1.687
	31	1.479	1.645	1.715	1.768	1.925	1.837	1.721	1.697
	32	.832	.624	.598	.571	.552	.568	.520	.505
.817	33	.720	.534	.573	.511	.419	.521	.488	.491
	34	.582	.531	.627	.647	.701	.568	.575	.608
	35	1.358	3.480	3.540	3.160	3.150	1.705	1.540	1.547
	36	1.889	3.580	3.100	2.760	3.015	1.650	1.497	1.513
	37	1.750	2.615	3.000	2.760	3.015	1.650	1.497	1.513
	38	1.670	2.205	2.815	2.760	3.065	1.650	1.502	1.519
	39	1.563	1.894	2.188	2.647	2.378	1.650	1.506	1.525
	40	-----	-----	1.802	1.924	1.845	1.628	1.530	1.542
	41	-----	1.594	1.715	1.762	1.739	1.814	-----	-----
	42	.891	.693	.675	.652	.643	.672	.612	.590
	43	.770	.586	.643	.624	.620	.620	.582	.582
	44	.699	.564	.675	.684	.676	.672	.677	.693
.946	45	.948	2.470	2.538	2.402	2.219	1.650	1.580	1.604
	46	1.872	3.260	2.489	2.181	1.930	1.512	1.446	1.478
	47	1.739	2.371	2.489	2.181	1.949	1.541	1.446	1.478
	48	1.634	2.087	2.464	2.181	1.949	1.512	1.440	1.473
	49	1.512	1.748	2.218	2.124	1.930	1.512	1.446	1.478
	50	1.446	1.674	1.878	2.095	1.949	1.512	1.451	1.484
	51	1.440	1.605	1.658	1.973	1.930	1.512	1.460	1.491
	52	1.423	1.565	1.600	1.825	1.801	1.512	1.460	1.491

TABLE I.- PRESSURE COEFFICIENTS - Continued

(d) $M = 0.60$, split flap off

$\frac{y}{b/2}$	Orifice number	Angle of attack, α , deg										
		-2.1	4.2	8.4	10.4	12.5	14.6	16.6	18.7	20.8	22.7	26.7
0.429	1	1.435	0.930	0.680	0.590	0.535	0.501	0.479	0.462	0.441	0.435	0.401
	2	1.486	.820	.577	.530	.480	.435	.445	.450	.443	.454	.460
	3	1.510	.800	.520	.530	.520	.539	.542	.573	.598	.650	.678
	4	.880	.915	2.065	2.381	2.542	2.570	2.457	2.395	2.178	2.050	1.879
	5	.761	1.920	2.977	2.735	2.519	2.375	2.161	2.052	2.000	1.962	1.859
	6			2.905	2.730	2.515	2.365	2.140	2.030	1.998	1.937	1.855
	7	1.015	1.730	2.247	2.757	2.517	2.364	2.143	2.052	1.999	1.962	1.855
	8	1.122	1.610	1.902	2.591	2.530	2.339	2.142	2.054	2.003	1.963	1.853
	9	1.170	1.560	1.783		2.570	2.365	2.142	2.056	2.010	1.964	1.853
	10	1.241	1.560	1.698	1.740	2.301	2.365	2.147	2.058	2.020	1.965	1.859
.558	11	1.450	.905	.661	.625	.539	.520	.487	.482	.478	.451	.450
	12	1.495	.790	.567	.548	.500	.479	.475	.463	.480	.470	.475
	13	1.525	.635	.527	.570	.510	.557	.583	.602	.640	.680	.715
	14	.615	1.145	2.370	2.580	2.360	2.185	2.157	1.947	1.895	1.840	1.800
	15	.740	1.980	3.062	2.463	2.179	2.042	2.000	1.902	1.863	1.830	1.795
	16	.883	1.910	2.970	2.463	2.142	2.020	1.950	1.898	1.860	1.820	1.780
	17	1.005	1.750	2.480	2.463	2.125	2.000	1.922	1.895	1.860	1.810	1.770
	18	1.110	1.650	1.955	2.431	2.123	2.000	1.927	1.895	1.859	1.810	1.795
	19	1.165	1.565	1.800	2.425	2.120	1.998	1.927	1.895	1.860	1.820	1.795
	20	1.190	1.560	1.742	2.159	2.119	1.998	1.928	1.900	1.862	1.820	1.797
	21	1.235	1.560	1.698	1.903	2.118	1.997	1.929	1.901	1.864		1.800
.688	22	1.460	.905	.673	.639	.598	.525	.523	.490	.490	.480	.445
	23				.583		.435	.435	.437	.575	.575	.582
	24	1.540	.600	.542	.583	.597	.580	.598	.622	.665	.682	.780
	25	.640	1.170	2.340	2.715	2.001	1.960	1.899	1.758	1.698	1.698	1.700
	26	.735	2.055	2.969	2.600	1.842	1.780	1.765	1.700	1.670	1.677	1.698
	27	.895	1.960	2.770	2.580	1.841	1.759	1.742	1.698	1.665	1.676	1.697
	28	1.000	1.780	2.335	2.580	1.855	1.770	1.740	1.698	1.670	1.676	1.697
	29	1.169	1.585	1.842	2.380	1.870	1.781	1.740	1.700	1.677	1.679	1.700
	30	1.185	1.565	1.739	1.945	1.860	1.781	1.742	1.700	1.682	1.680	1.701
	31	1.235	1.565	1.682	1.710	1.850	1.742	1.743	1.715	1.698	1.679	1.699
	.817	32	1.399	.865	.647	.638	.575	.579	.543	.541	.542	.542
33		1.525	.780	.562	.581	.533	.542	.507	.507	.500	.521	.540
34		1.527	.635	.530	.630	.580	.580	.542	.560	.598	.625	.705
35		.585	1.370	2.601	2.810	2.660	2.298	1.580	1.530	1.538	1.582	1.610
36		.733	2.060	2.630	2.600	2.501	1.900	1.543	1.507	1.525	1.567	1.605
37		.883	1.940	2.581	2.580	2.541	1.899	1.540	1.505	1.523	1.567	1.605
38		1.025	1.810	2.525	2.560	2.570	1.925	1.540	1.507	1.525	1.568	1.610
39		1.111	1.680	2.261	2.600	2.680	1.955	1.542	1.510	1.537	1.568	1.610
40		1.170	1.565	1.700	2.040	1.542	1.623	1.546	1.530	1.538	1.569	1.610
41				1.462	1.920	1.560	1.582	1.563	1.535	1.550	1.568	1.599
.946		42	1.465	.960	.755	.780	.685	.679	.679	.673	.627	.630
	43	1.545	.835	.642	.650	.595	.610	.601	.610	.600	.600	.620
	44	1.533	.675	.590	.635	.641	.679	.633	.670	.680	.720	.783
	45	.699	1.010	1.855	1.883	2.115	2.000	1.503	1.540	1.580	1.578	1.542
	46	.783	1.970	2.300	1.925	2.095	1.927	1.415	1.421	1.482	1.498	1.525
	47				1.920	2.085	1.954	1.435	1.420	1.483	1.497	1.518
	48	1.050	1.750	2.387	1.923	2.095	1.985	1.415	1.420	1.482	1.498	1.525
	49	1.145	1.610	2.150	1.959	2.115	2.050	1.416	1.423	1.483	1.500	1.530
	50	1.170	1.555	1.900	1.959	2.113	1.899	1.418	1.440	1.484	1.501	1.540
	51	1.220	1.530	1.675	1.915	2.000	1.700	1.420	1.441	1.485	1.502	1.559
	52	1.240	1.530	1.545	1.900	1.801	1.630	1.430	1.455	1.486	1.504	1.561

TABLE I.- PRESSURE COEFFICIENTS - Continued

(e) $M = 0.70$, split flap off

$\frac{y}{b/2}$	Orifice number	Angle of attack, α , deg											
		-2.1	4.2	8.4	10.5	12.5	14.6	16.7	18.7	20.7	22.7	24.7	26.7
0.429	1	1.560	0.975	0.633	0.658	0.620	0.577	0.540	0.520	0.505	0.482	0.465	0.450
	2	1.597	.850	.520	.561	.542	.510	.500	.495	.498	.490	.485	.493
	3	1.604	.720	.450	—	.560	.566	.565	.592	.612	.632	.660	.678
	4	1.000	.955	1.672	2.172	2.350	2.480	2.518	2.485	2.425	1.903	2.002	1.958
	5	.825	1.990	—	2.828	2.508	2.375	2.190	2.090	2.000	1.775	1.950	1.942
	6	1.060	—	2.760	2.811	2.505	2.340	2.192	2.089	1.995	1.770	1.945	1.940
	7	—	1.790	2.705	2.826	2.495	2.326	2.193	2.092	2.010	1.774	1.945	1.940
	8	1.200	1.710	1.972	2.645	2.478	2.324	2.200	2.093	2.020	1.774	1.945	1.940
	9	1.255	1.640	1.808	2.354	2.472	2.305	2.215	2.098	2.030	1.775	1.947	1.942
	10	1.330	1.640	1.737	1.851	2.430	2.290	2.200	2.099	1.800	—	1.952	1.943
.558	11	1.562	.950	.610	.658	.627	.588	.550	.535	.520	.507	.492	.481
	12	1.620	.812	.510	.606	.564	.544	.515	.520	.517	.512	.518	.522
	13	1.640	.672	.445	.606	.601	.601	.610	.640	.660	.682	.718	.525
	14	.695	1.125	1.922	2.332	2.285	2.347	2.315	1.992	1.970	1.923	1.903	1.900
	15	.745	2.050	2.740	2.400	2.140	2.312	2.015	1.960	1.940	1.910	1.898	1.895
	16	.958	1.990	2.745	2.415	2.142	—	1.975	1.930	1.935	1.905	1.895	1.895
	17	1.080	1.835	2.635	2.415	2.160	—	1.980	1.932	1.935	1.900	1.888	1.895
	18	1.184	1.735	2.298	2.413	2.200	2.311	1.990	1.940	1.935	1.900	1.890	1.895
	19	1.233	1.650	1.955	2.380	2.200	2.313	1.990	1.937	1.934	1.900	1.895	1.895
	20	1.235	1.650	1.750	2.302	2.182	2.310	1.995	1.955	1.935	1.905	1.895	1.897
	21	1.330	1.645	1.703	2.146	2.160	—	1.999	1.955	1.938	1.910	1.898	1.897
.688	22	1.580	.948	.610	.696	.633	.615	.575	.570	.550	.535	.515	.505
	23	—	.686	.492	.594	.614	.610	—	.622	.605	.610	.610	.628
	24	1.635	.653	.455	.588	.645	.623	.636	—	.698	—	.760	.812
	25	.685	1.160	1.942	2.439	2.608	2.010	2.045	1.916	1.820	1.878	1.820	1.840
	26	.795	2.108	2.702	2.582	2.706	1.828	1.835	1.800	1.795	1.800	1.815	1.838
	27	.960	2.077	2.645	2.569	2.700	1.819	1.833	1.795	1.795	1.797	1.815	1.838
	28	1.065	1.938	—	2.569	2.740	1.836	1.830	1.793	1.795	1.795	1.813	1.837
	29	1.240	1.685	2.120	2.465	2.630	1.843	1.810	1.787	1.795	1.795	1.815	1.837
	30	1.330	1.662	1.810	2.144	1.860	1.850	1.811	1.790	1.797	1.797	1.815	1.837
	31	1.360	1.660	1.685	1.812	1.828	1.852	1.830	1.792	1.799	1.795	1.815	1.837
	.817	32	1.540	.923	.615	.690	.647	.646	.625	.610	.605	.585	.570
33		1.668	.817	.512	.628	.577	.597	.565	.570	.565	.565	.570	.575
34		1.660	.646	.458	.628	.610	.636	.602	.610	.618	.680	.702	.750
35		.518	1.368	2.270	2.728	2.530	2.298	1.680	1.635	1.680	1.725	1.752	1.767
36		.775	2.130	2.540	2.498	2.415	2.115	1.630	1.630	1.660	1.717	1.750	1.765
37		.957	2.075	2.508	2.512	2.415	2.120	1.625	1.623	1.660	1.715	1.748	1.763
38		1.085	1.895	2.440	2.484	2.422	2.170	1.625	1.628	1.660	1.715	1.745	1.763
39		1.190	1.776	2.350	—	2.455	2.185	1.630	1.630	1.663	1.715	1.748	1.766
40		1.285	1.656	1.906	2.296	2.325	1.660	1.640	1.632	1.665	1.717	1.750	1.766
41		—	—	—	1.910	—	—	1.648	1.640	1.658	1.690	1.718	1.745
.946		42	1.597	1.003	.703	.822	.740	.730	.738	.720	.700	.685	.675
	43	1.678	.870	.595	—	.656	.678	.670	.670	.665	.660	.670	.664
	44	1.650	.715	.540	.631	.669	.708	.698	.720	.740	.765	.805	.832
	45	.760	1.042	1.650	1.757	1.888	2.132	1.605	1.680	1.720	1.715	1.678	1.682
	46	.870	2.146	2.135	1.910	1.920	2.127	1.565	1.545	1.585	1.620	1.640	1.665
	47	—	—	2.134	1.980	1.922	2.100	1.485	—	1.585	1.617	1.635	1.660
	48	1.113	1.868	2.180	1.955	1.910	2.180	1.520	1.555	1.595	1.620	1.640	1.666
	49	1.190	1.708	2.131	1.965	1.910	2.253	1.525	1.556	1.600	1.625	1.641	1.670
	50	1.280	1.633	2.025	1.965	1.918	2.100	1.530	1.560	1.602	1.630	1.648	1.675
	51	1.333	1.613	1.866	1.950	1.912	—	1.528	1.560	1.605	1.632	1.655	1.678
	52	1.345	1.600	1.682	1.950	1.910	1.850	1.535	1.562	1.605	1.636	1.660	1.687

TABLE I.- PRESSURE COEFFICIENTS - Continued

(f) $M = 0.80$, split flap off

$\frac{y}{b/2}$	Orifice number	Angle of attack, α , deg									
		-2.1	4.2	8.4	10.5	12.6	14.7	16.7	18.7	20.7	22.7
0.429	1	1.606	1.031	0.780	0.707	0.663	0.625	0.605	0.558	0.542	0.526
	2	1.638	.910	.673	.615	.585	.543	.539	.539	.539	.525
	3	1.652	.695	.600	.579	.585	.560	.561	.572	.618	.625
	4	.960	.930	1.501	1.820	2.086	2.125	2.267	2.290	2.270	2.202
	5	.872	2.000	2.693	2.902	2.728	2.438	2.234	2.161	2.088	2.072
	6	1.062	1.941	2.710	2.982	2.698	2.385	2.206	2.149	2.065	2.052
	7	1.128	1.855	2.721	2.970	2.635	2.378	2.209	2.120	2.033	2.057
	8	1.246	1.784	2.602	2.850	2.542	2.370	2.196	2.136	2.053	2.052
	9	1.330	1.760	1.979	2.687	2.537	2.369	2.198	2.150	2.041	2.052
	10	1.360	1.785	2.030	2.120	2.314	2.310	2.209	2.136	2.072	2.057
.558	11	1.645	.992	.762	.707	.663	.628	.606	.558	.558	.542
	12	1.690	.885	.662	.633	.600	.658	.553	.548	.550	.546
	13	1.688	.700	.615	.595	.610	.620	.620	.641	.643	.695
	14	.719	1.083	1.742	2.032	2.245	2.320	2.242	2.247	2.101	1.992
	15	.830	2.040	2.800	2.967	2.363	2.200	2.037	2.018	1.998	1.985
	16	1.060	2.100	2.910	3.008	2.310	2.093	1.958	1.955	1.988	1.981
	17	1.129	1.941	2.849	2.970	2.290	2.084	1.967	1.968	2.003	1.980
	18	1.244	1.832	2.722	2.865	2.290	2.121	1.975	1.982	1.980	1.981
	19	1.292	1.792	2.667	2.768	2.290	2.166	2.022	1.987	1.978	1.980
	20	1.342	1.749	1.830	2.528	2.282	2.178	2.037	1.999	1.983	1.981
	21	1.354	1.752	1.825	2.379	2.207	2.178	2.055	1.997	1.989	1.990
.688	22	1.665	.990	.830	.702	.698	.628	.620	.611	.563	.588
	23	---	.698	.659	.618	.638	.620	.610	.620	.582	.622
	24	1.700	.658	.620	.618	.638	.628	.628	.645	.702	.742
	25	.705	1.110	1.798	2.125	2.037	2.127	2.046	2.004	1.940	1.946
	26	.840	2.127	2.900	2.379	2.008	2.110	1.866	1.876	1.928	1.949
	27	1.003	2.127	2.965	2.370	2.008	2.105	1.860	1.866	1.882	1.918
	28	1.118	2.040	2.920	2.341	2.023	1.912	1.840	1.856	1.882	1.915
	29	1.280	1.790	2.773	2.332	2.080	1.953	1.774	1.782	1.880	1.907
	30	1.342	1.795	2.375	2.290	2.094	1.960	1.864	1.854	1.882	1.913
	31	1.358	1.795	1.893	2.225	2.084	1.955	1.864	1.858	1.883	1.907
.817	32	1.619	.960	.805	.753	.715	.685	.680	.632	.625	.620
	33	1.756	.858	.679	.661	.657	.620	.613	.608	.596	.627
	34	1.717	.700	.615	.617	.657	.626	.623	.630	.655	.715
	35	.660	1.318	2.097	2.193	2.502	1.967	1.748	1.622	1.803	1.868
	36	.818	2.162	2.913	2.120	2.570	1.898	1.695	1.730	1.790	1.846
	37	.990	2.240	2.975	2.120	2.570	1.883	1.684	1.722	1.785	1.840
	38	1.100	2.075	2.921	2.120	2.606	1.893	1.686	1.722	1.785	1.836
	39	1.243	1.900	2.848	2.150	2.622	1.928	1.716	1.728	1.786	1.836
	40	1.331	1.780	2.260	2.107	2.000	1.781	1.702	1.730	1.790	1.870
	41	---	---	1.893	1.981	1.830	1.684	1.687	1.722	---	---
.946	42	1.700	1.040	.900	.838	.808	.776	.734	.728	.715	.714
	43	1.796	.915	.760	.719	.740	.701	.701	.701	.700	.702
	44	1.722	.723	.690	.682	.725	.703	.706	.720	.728	.803
	45	.785	1.039	1.641	1.822	2.006	1.747	1.668	1.750	1.810	1.828
	46	.884	2.279	2.307	2.380	2.198	1.794	1.620	1.728	1.702	1.746
	47	---	---	---	2.342	2.198	1.888	1.628	---	---	1.721
	48	1.170	2.132	2.267	2.342	2.219	---	1.602	1.660	1.707	1.746
	49	1.283	2.083	2.242	2.300	2.230	1.822	1.606	1.655	1.707	1.760
	50	1.343	1.708	2.195	2.281	2.241	1.805	1.610	1.663	1.715	1.726
	51	1.361	1.670	2.110	2.005	2.165	1.782	1.620	1.668	1.722	1.772
	52	---	1.655	2.023	1.703	2.010	1.712	1.620	1.666	1.722	1.772

TABLE I.- PRESSURE COEFFICIENTS - Continued

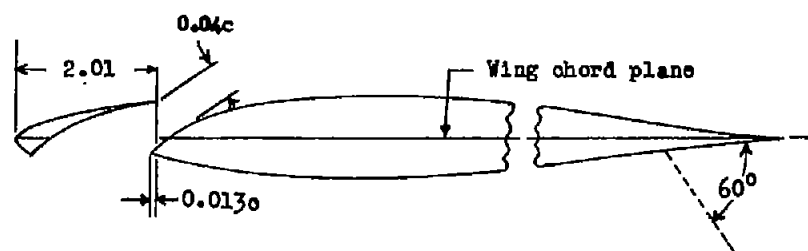
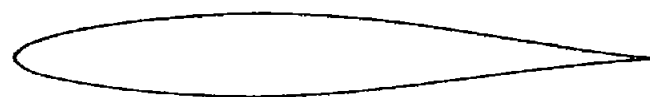
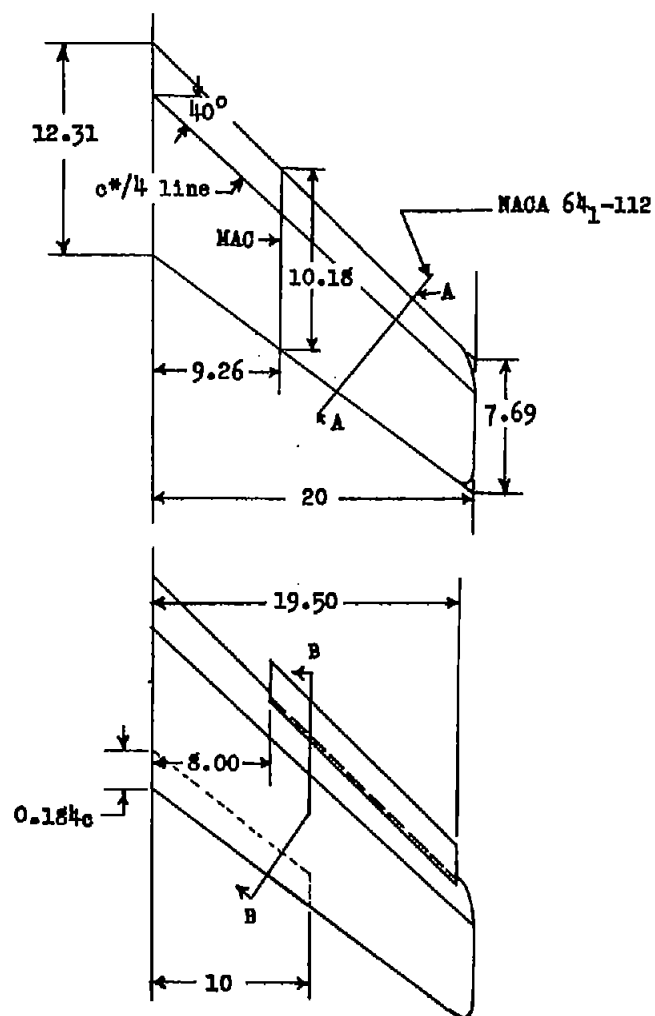
(g) $M = 0.84$, split flap off

$\frac{y}{b/2}$	Orifice number	Angle of attack, α , deg						
		-2.1	4.2	8.4	10.5	12.6	14.7	16.7
0.429	1	1.630	1.068	0.822	0.759	0.675	0.622	0.618
	2	1.680	.950	.707	.627	.601	.564	.561
	3	1.642	.808	.620	.590	.572	.572	.580
	4	.807	.922	1.198	1.660	1.821	2.090	1.720
	5	.978	1.926	2.523	2.723	2.793	2.396	2.218
	6	---	1.885	2.600	2.780	2.837	2.380	2.158
	7	1.160	1.844	2.600	2.770	2.837	2.380	2.221
	8	1.288	1.780	2.485	2.661	2.780	2.374	2.222
	9	1.430	1.760	---	2.661	2.737	2.374	---
	10	1.418	1.820	2.023	2.170	2.380	2.315	2.230
.558	11	1.670	1.038	.803	.759	.690	.648	.638
	12	1.715	.921	.707	.627	.601	.602	.581
	13	1.672	.762	.620	.610	.601	.610	.640
	14	.718	1.042	1.599	1.863	2.058	2.200	2.197
	15	.860	1.947	2.599	2.775	2.423	2.182	2.133
	16	1.032	2.100	2.701	2.827	2.320	2.138	2.062
	17	1.175	1.942	2.659	2.827	2.280	---	2.045
	18	1.270	1.892	2.599	2.775	2.247	2.120	2.045
	19	1.337	1.857	2.587	2.723	2.239	2.135	2.058
	20	1.399	1.857	2.401	2.663	2.239	2.157	2.067
	21	1.415	1.895	2.055	2.663	2.239	2.172	2.085
.688	22	1.690	.962	.822	.759	.728	.690	.646
	23	---	.742	.641	.620	.623	.620	.618
	24	1.670	.722	.630	.629	.630	.680	.665
	25	.733	1.067	1.625	1.880	2.002	2.104	2.126
	26	.859	2.041	2.678	2.342	2.119	1.957	1.910
	27	1.034	2.225	2.761	2.280	2.095	1.956	1.905
	28	1.138	2.079	2.720	2.280	2.089	1.956	1.910
	29	1.320	1.919	2.621	2.200	2.089	1.980	1.938
	30	1.377	1.907	2.577	2.187	2.089	1.980	1.939
	31	1.420	1.927	2.539	2.187	2.089	1.980	1.943
	32	1.611	.920	.803	.763	.743	.724	.692
.817	33	1.782	.888	.721	.675	.657	.650	.638
	34	1.720	.742	.645	.647	.639	.650	.645
	35	.675	1.260	1.903	2.062	2.150	1.957	1.833
	36	.840	2.130	2.730	1.978	2.139	1.843	1.770
	37	1.021	2.218	2.775	2.005	2.135	1.833	1.759
	38	1.155	2.202	2.775	2.020	2.135	1.843	1.759
	39	1.265	2.046	2.697	2.037	2.129	1.859	1.762
	40	1.365	1.905	2.521	2.060	2.127	1.833	1.760
	41	---	---	2.047	2.037	---	1.859	---
	42	1.743	.712	.902	.859	.838	.842	.800
	43	1.839	.758	.799	.759	.742	---	.726
.946	44	1.681	.788	.721	.735	.742	.750	.742
	45	.813	1.020	1.540	1.761	1.823	1.800	1.735
	46	1.134	2.182	2.155	2.570	2.200	1.878	1.693
	47	---	---	---	---	---	---	---
	48	1.203	2.260	2.099	2.560	2.139	1.878	1.690
	49	1.333	2.140	2.099	2.440	2.150	1.920	1.705
	50	1.444	1.992	2.113	2.423	2.056	1.930	1.707
	51	1.430	1.790	2.085	2.220	1.890	1.800	1.707
	52	1.468	1.580	2.038	---	1.890	1.765	1.706

TABLE I.- PRESSURE COEFFICIENTS - Concluded

(h) $M = 0.91$, split flap off

$\frac{y}{b/2}$	Orifice number	Angle of attack, α , deg		
		4.2	8.4	10.6
0.429	1	1.132	0.900	0.830
	2	1.049	.745	.720
	3	.910	.685	.642
	4	.817	1.120	1.320
	5	1.690	2.130	2.300
	6	1.714	2.238	2.403
	7	1.745	2.257	2.419
	8	1.738	2.178	2.359
	9	1.717	2.000	2.210
	10	1.771	1.538	1.910
.558	11	1.149	.920	.825
	12	1.040	.820	.730
	13	.883	.645	.641
	14	.922	1.285	1.460
	15	1.713	2.190	2.358
	16	1.853	2.300	2.450
	17	1.820	2.333	2.437
	18	1.821	2.265	2.430
	19	1.796	2.210	2.380
	20	1.803	2.180	2.355
	21	1.827		2.300
.688	22	1.148	.925	.830
	23		.695	.690
	24	.851	.695	.675
	25	.925	1.305	1.240
	26	1.778	2.220	2.401
	27	1.950	2.340	2.480
	28	1.891	2.340	2.483
	29	1.855	2.279	2.430
	30	1.870	2.262	2.430
	31	1.880	2.238	2.430
.817	32	1.111	.940	.880
	33	1.024	.835	.785
	34	.864	.658	.690
	35	1.070	1.460	1.690
	36	1.801	2.163	2.419
	37	1.963	2.340	2.487
	38	1.963	2.340	2.487
	39	1.955	2.340	2.480
	40	1.920	2.319	2.450
	41			
.946	42	1.173	1.042	.960
	43	1.050	.916	.803
	44	.891	.795	.759
	45	.915	1.242	1.400
	46	1.865	2.290	2.453
	47			
	48	2.024	2.410	2.520
	49	2.038	2.410	2.507
	50	2.010	2.400	2.488
	51	2.010	2.400	2.475
	52	2.015	2.400	2.450



Section B - B (enlarged)

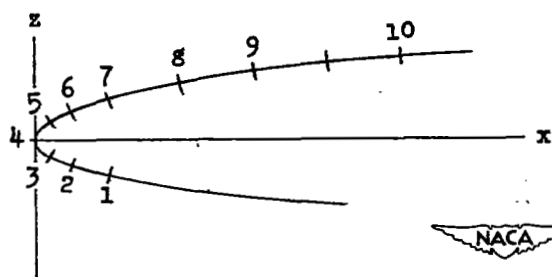
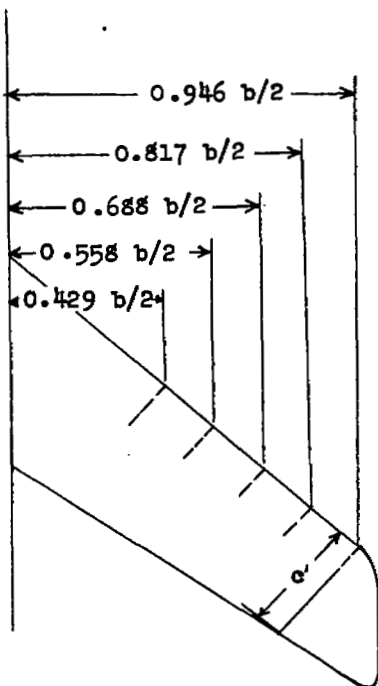


Dimensions given in inches unless otherwise noted

(a) Details of wing and slat.

Figure 1.- Sketch of 40° sweptback wing.

x/c'	z/c'	Orifice Number for $y/b/2$				
		.429	.558	.688	.817	.946
0.050	-0.119	1	11	22	32	42
.025	-.087	2	12	23	33	43
.010	-.059	3	13	24	34	44
0	0	4	14	25	35	45
.010	.064	5	15	26	36	46
.025	.098	6	16	27	37	47
.050	.136	7	17	28	38	48
.100	.189	8	18	—	39	49
.150	.227	9	19	29	—	50
.200	.257	—	20	30	40	51
.250	.277	10	21	31	41	52



(b) Orifice locations.

Figure 1.- Concluded.

CONFIDENTIAL



(a) Top view.

Figure 2.- Leading-edge slat mounted on 40° sweptback wing.



(b) Bottom view.

Figure 2.- Concluded.

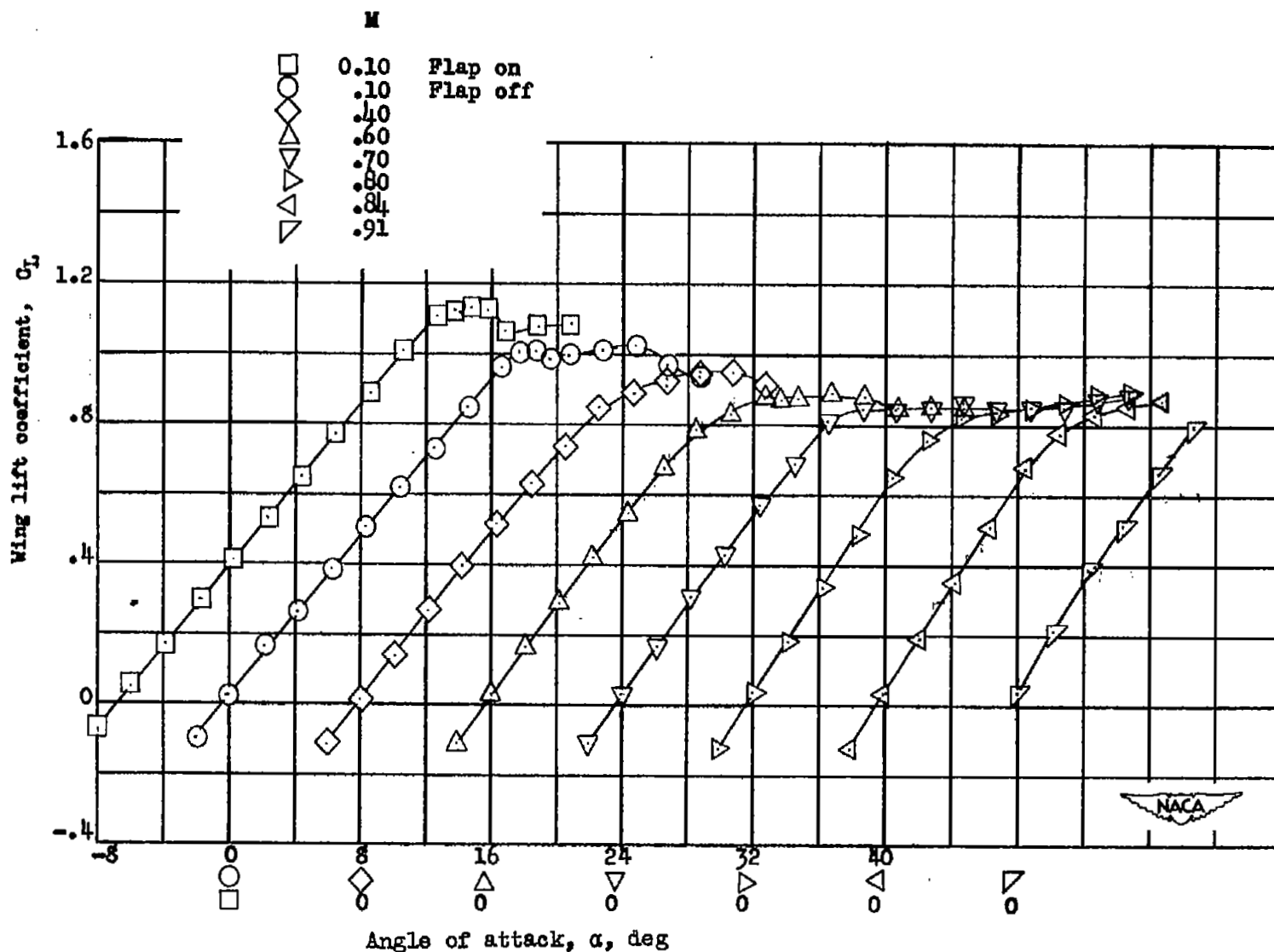


Figure 3.- Lift characteristics of 40° sweptback wing at various Mach numbers. 0.22c slat retracted.

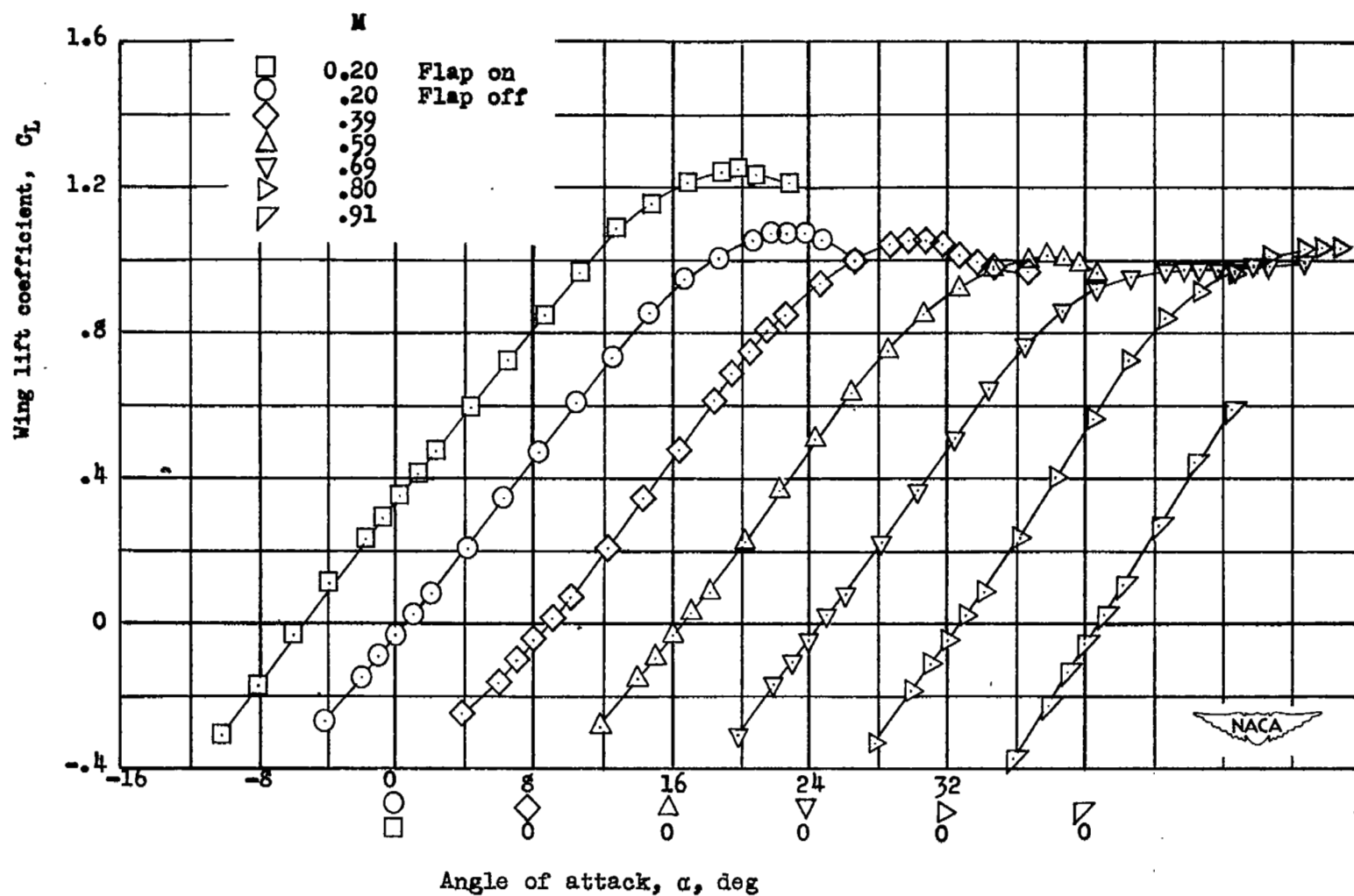


Figure 4.- Lift characteristics of 40° sweptback wing at various Mach numbers. 0.22c slat extended.

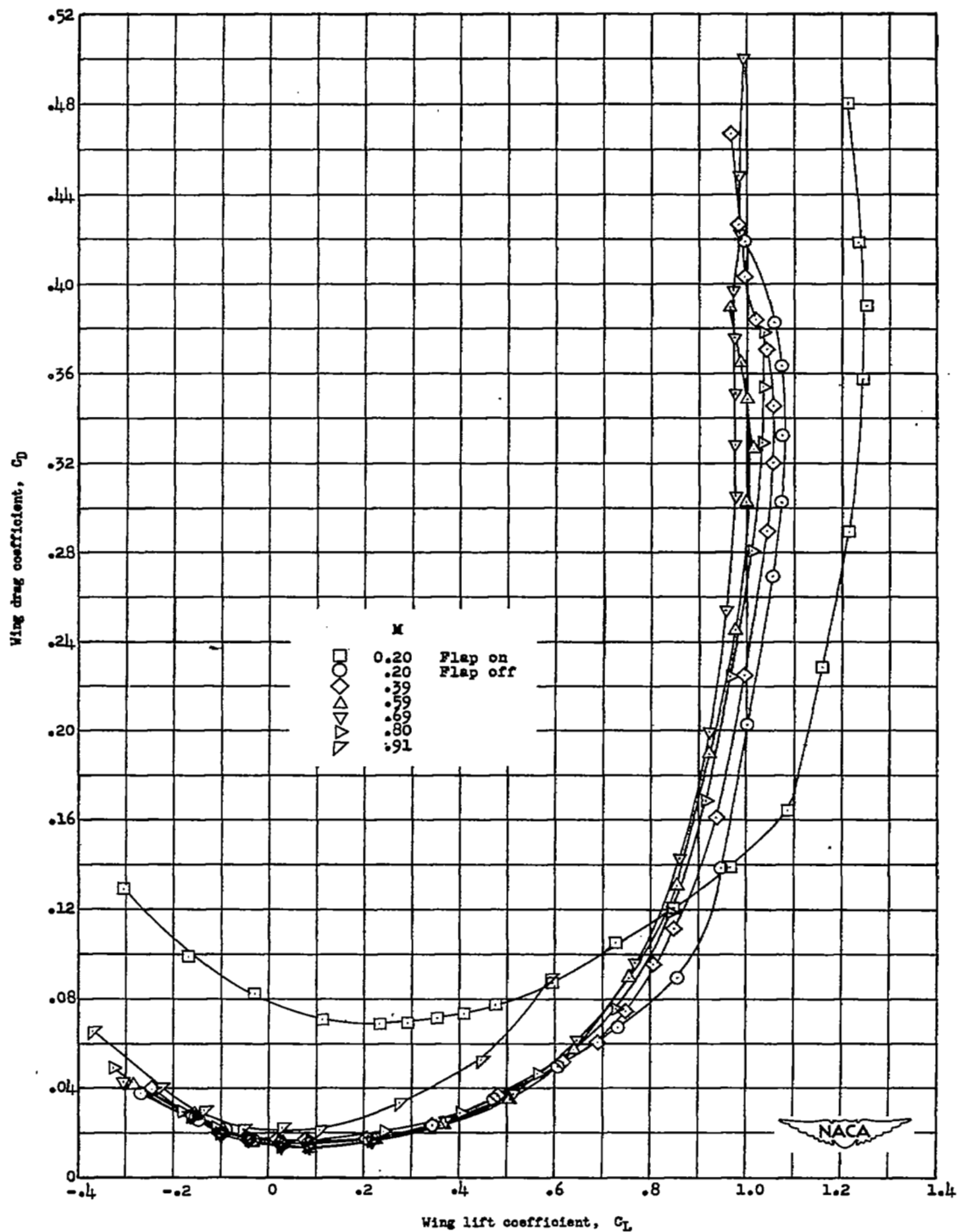


Figure 5.- Drag characteristics of 40° sweptback wing at various Mach numbers. 0.22c slat extended.

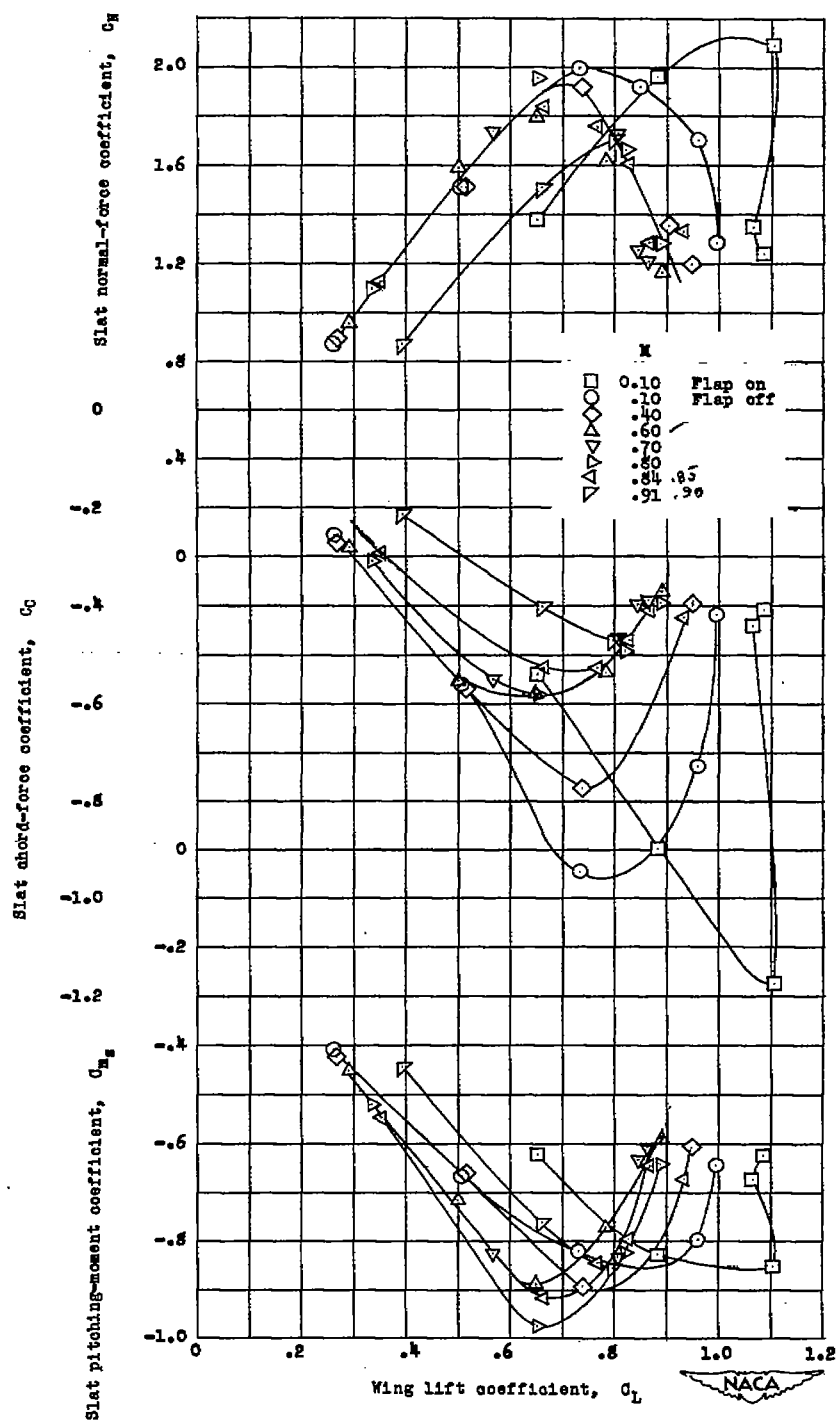


Figure 6.- Variation of integrated slat normal-force, chord-force, and pitching-moment coefficients with wing lift coefficient for various Mach numbers. 0.22c slat retracted.

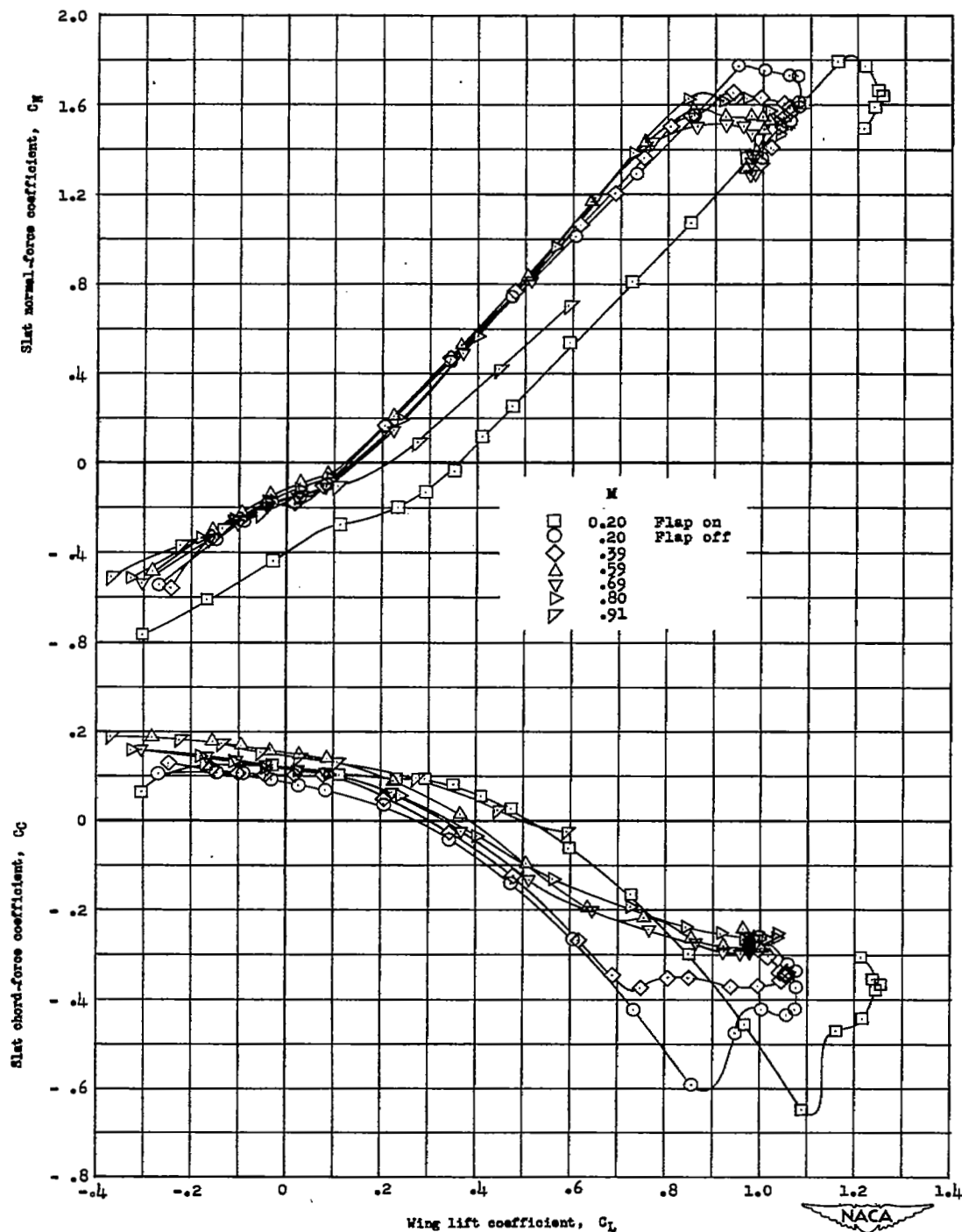


Figure 7.- Variation of slat normal-force and chord-force coefficients with wing lift coefficient for various Mach numbers. 0.22c slat extended.

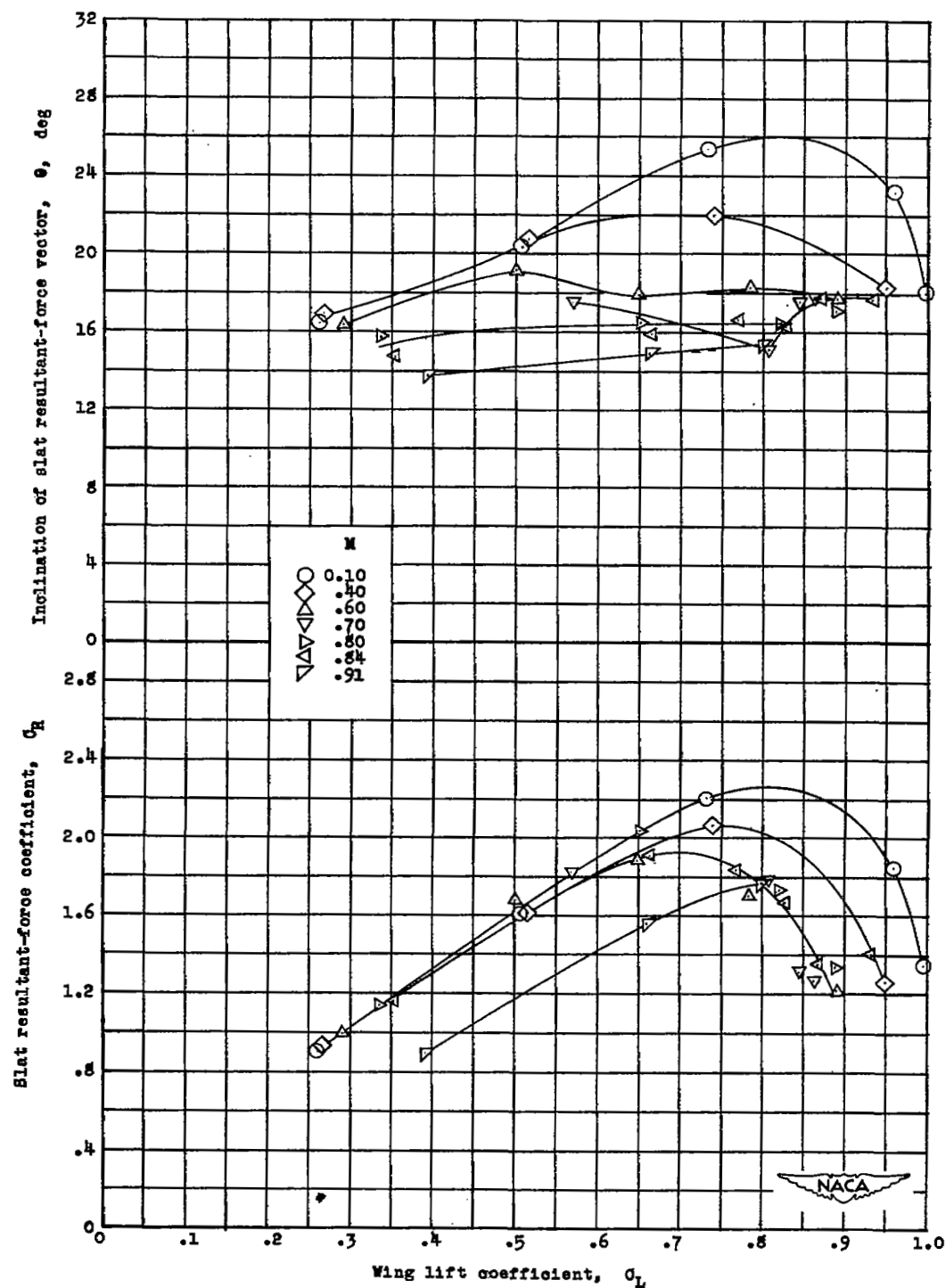


Figure 8.- Magnitude and inclination of slat resultant-force coefficient.
0.22c slat retracted.

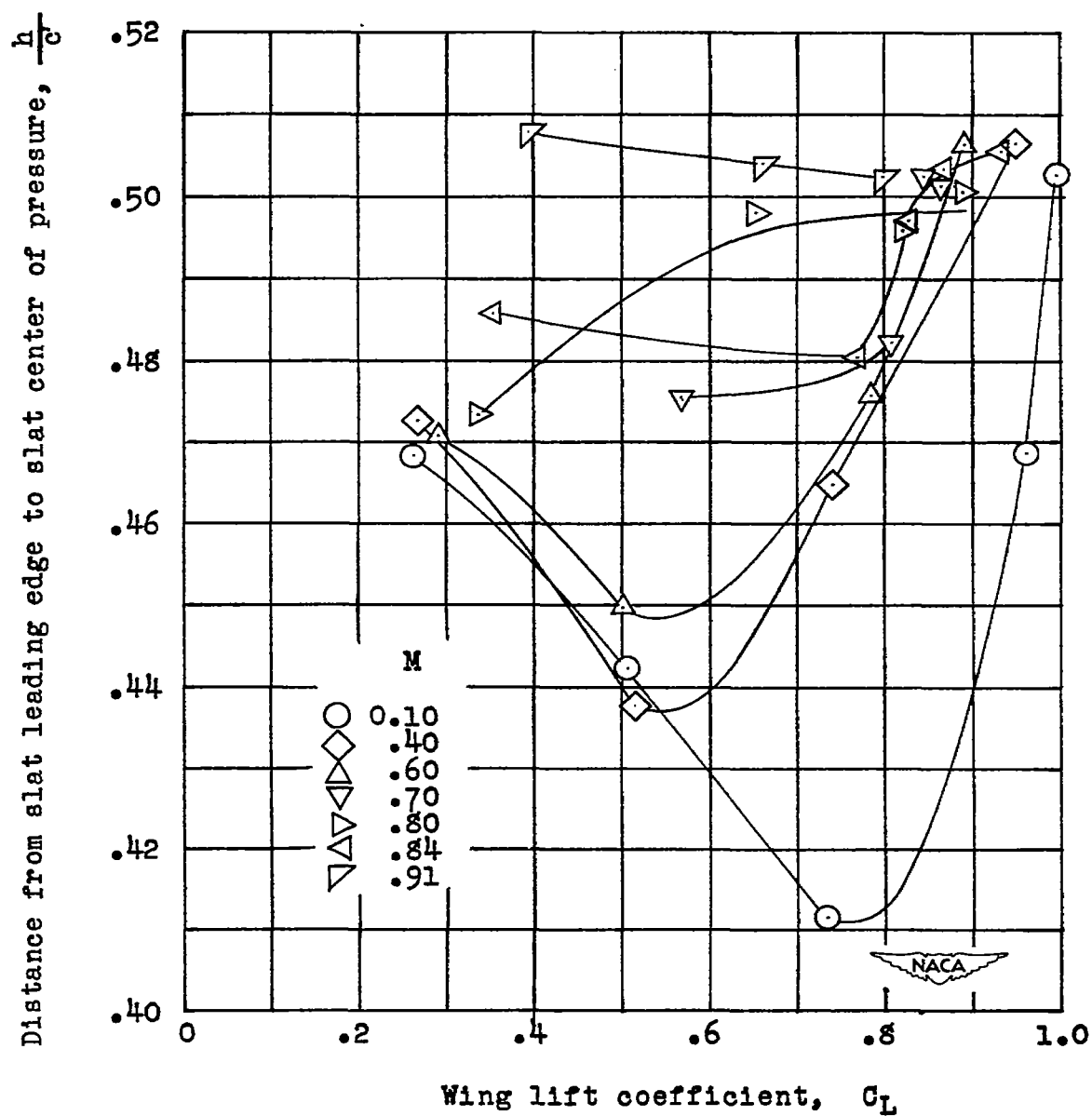
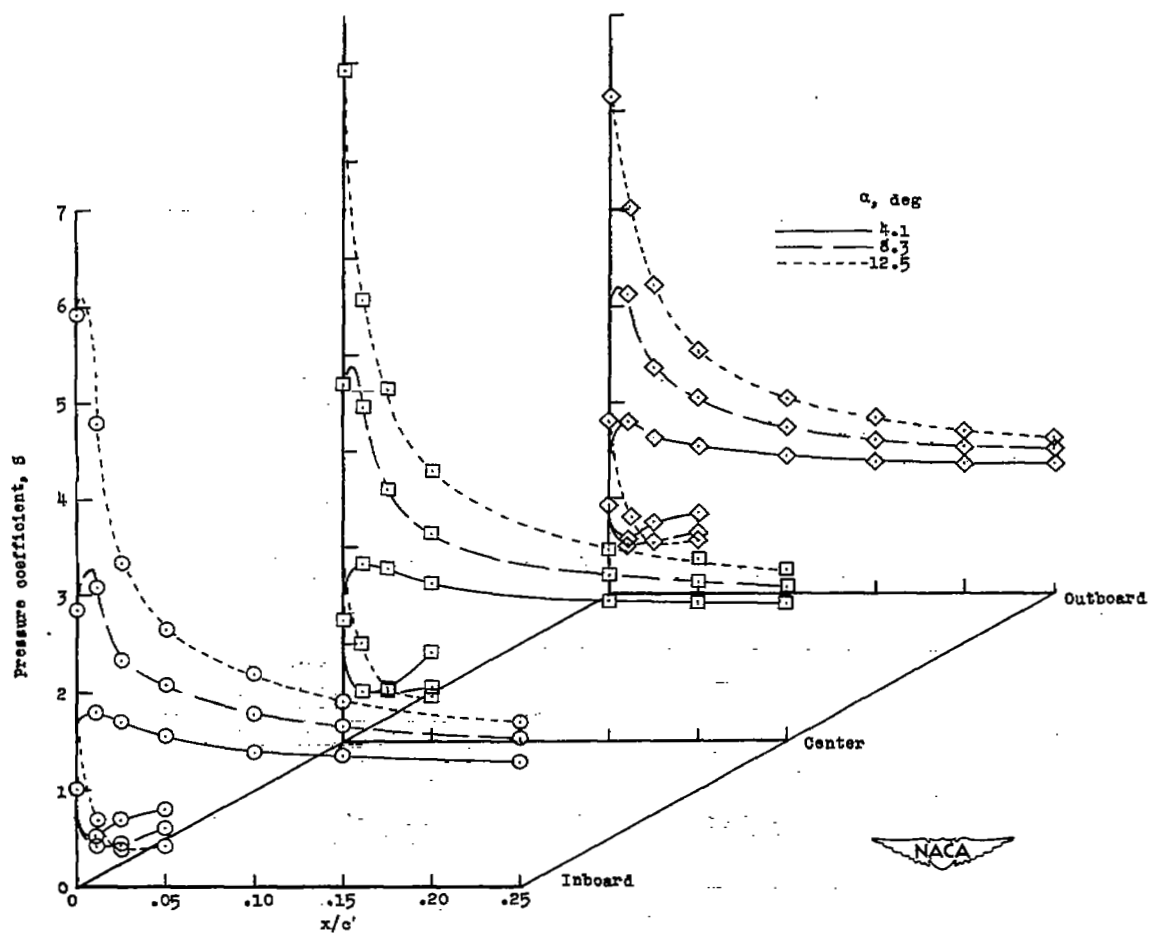
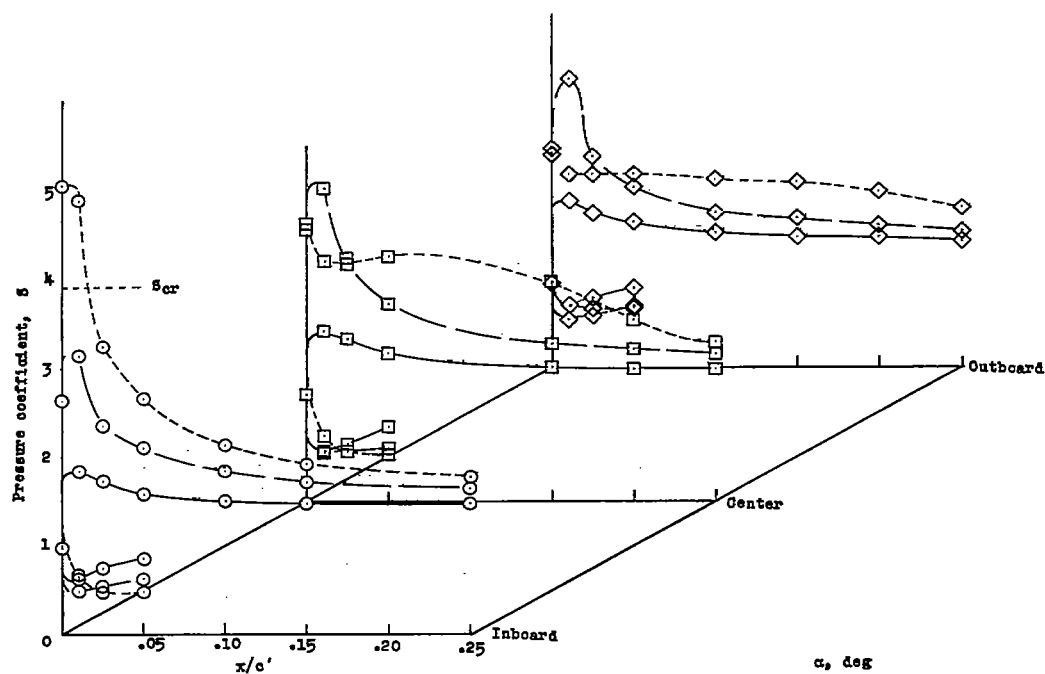


Figure 9.- Variation of center of pressure of slat load with wing lift coefficient. 0.22c slat retracted.

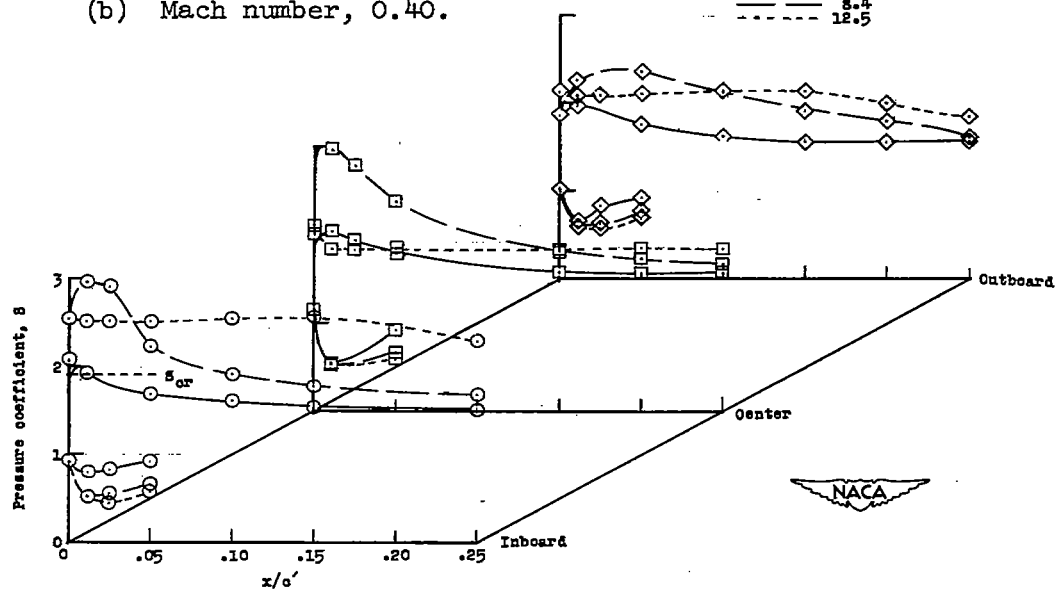


(a) Mach number, 0.10.

Figure 10.- Comparison of pressure distributions over retracted slat at several Mach numbers.

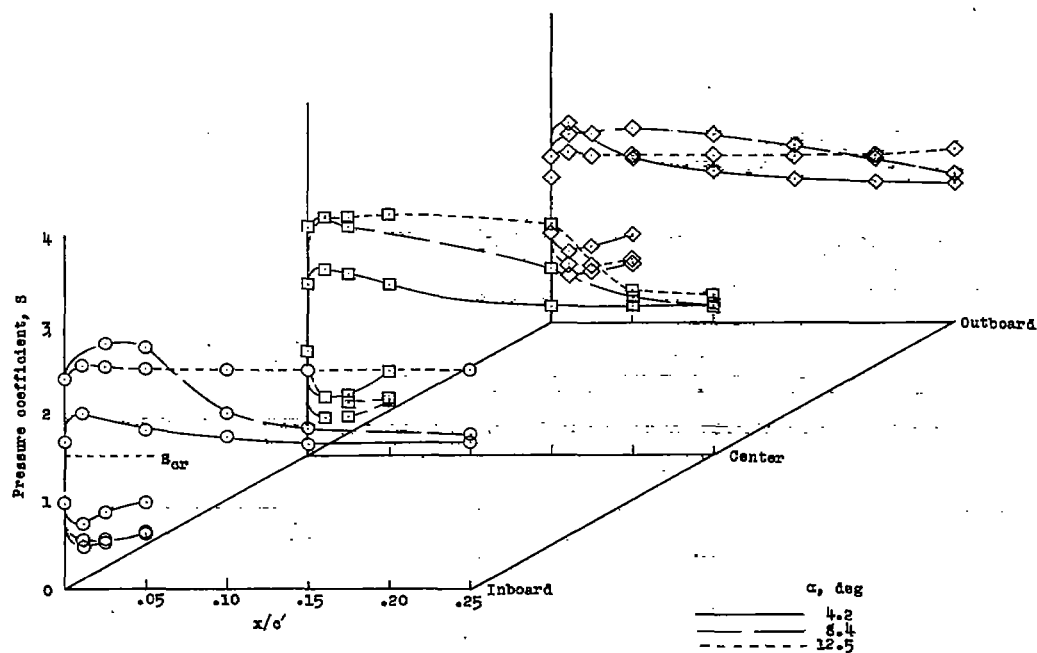


(b) Mach number, 0.40.

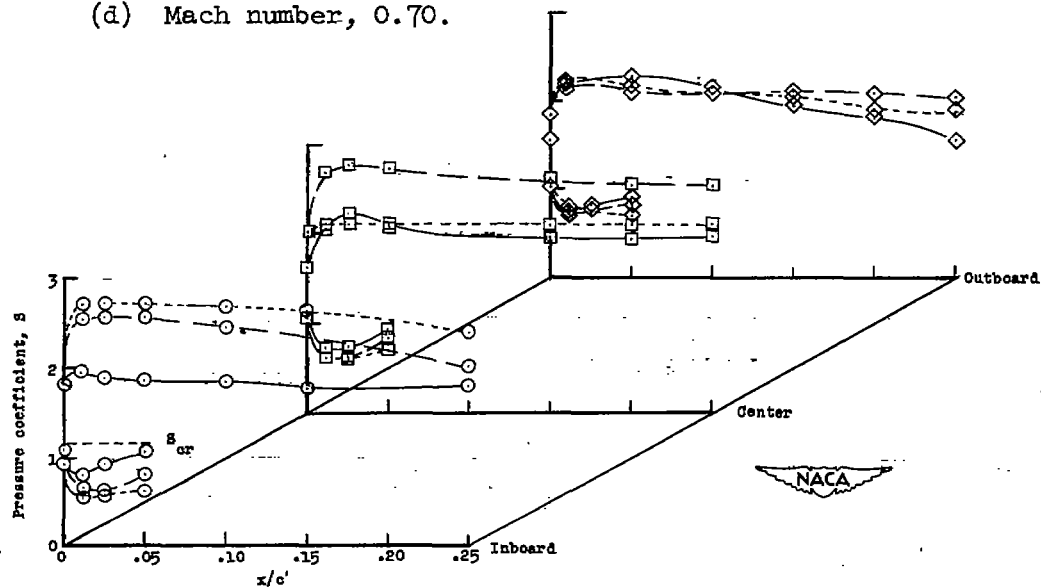


(c) Mach number, 0.60.

Figure 10.- Continued.



(d) Mach number, 0.70.



(e) Mach number, 0.84.

Figure 10.- Concluded.

SECURITY INFORMATION

